Edinburgh Research Explorer

The role of tonic glycinergic conductance in cerebellar granule cells signalling and the effect of gain-of-function mutation

The role of tonic glycinergic conductance in cerebellar granule cells signalling and the effect of gain-of-function mutation

Short title: Impact of T258F mutation of glycine receptor on cerebellar signalling.

Catherine McLaughlin[1], John Clements[2], Ana-Maria Oprişoreanu[3], Sergiy Sylantyev[4]*

[1] – Gene Therapy Group, The Roslin Institute, University of Edinburgh, Easter Bush, Midlothian EH25 9RG, UK.

[2] – The John Curtin School of Medical Research, Australian National University, 131 Garran Road, Canberra ACT 2601, Australia.

[3] – Center for Discovery Brain Sciences, University of Edinburgh, 49 Little France Crescent, Edinburgh EH16 4SB, UK.

[4] – Center for Clinical Brain Sciences, University of Edinburgh, 49 Little France Crescent, Edinburgh EH16 4SB, UK.

* – Corresponding author: s.sylantyev@ed.ac.uk

Key points

- A T258F mutation of the glycine receptor increases the receptor affinity to endogenous agonists, modifies single-channel conductance and shapes response decay kinetics.

- Glycine receptors of cerebellar granule cells play their functional role not continuously, but when granule cell layer starts receiving high amount of excitatory inputs.

- Despite their relative scarcity, tonically active glycine receptors of cerebellar granule cells make a significant impact on action potential generation, inter-neuronal crosstalk, and modulate synaptic plasticity in neural networks; extracellular glycine increases probability of postsynaptic response occurrence acting at NMDA receptors and decreases this probability acting at glycine receptors.

- Tonic conductance through glycine receptors of cerebellar granule cells is a yet undiscovered element of bi-phasic mechanism which regulates processing of sensory inputs in the cerebellum.

- T258F point mutation disrupts this bi-phasic mechanism, thus illustrating possible role of the gain-of-function mutations of glycine receptor in development of neural pathologies.

Abstract

Functional glycine receptors (GlyRs) were repeatedly detected in cerebellar granule cells (CGCs), where they deliver exclusively tonic inhibitory signalling. The functional role of this signaling, however, remains unclear. Apart from that, there is accumulating evidence of the important role of GlyRs of cerebellar structures in development of neural pathologies such as hyperekplexia, which can be triggered by GlyR gain-of-function mutations.

In this research we initially tested functional properties of GlyRs, carrying the yet understudied T258F gain-of-function mutation, to find that this mutation makes significant modifications in GlyR response to endogenous agonists. Next, we clarified the role of tonic GlyR conductance in neuronal signalling generated by single CGC and by neural networks in cell cultures and in living cerebellar tissue of C57Bl-6J mice. We found that GlyRs of CGC deliver a significant amount of tonic inhibition not continuously, but when cerebellar granule layer starts receiving substantial excitatory input. Under these conditions tonically active GlyRs become a part of neural signalling machinery allowing generation of action potentials (APs) bursts of limited length in response to sensory-evoked signals. GlyRs of CGCs support a biphasic modulatory mechanism which enhances AP firing when excitatory input intensity is low, but suppresses it when excitatory input rises to a certain critical level. This enables one of the key functions of the CGC layer: formation of sensory representations and their translation into motor output. Finally, we have demonstrated that T258F mutation in CGC GlyRs modifies single-cell and neural network signalling, and brakes a biphasic modulation of AP-generating machinery.

Key words: glycine receptor; gain-of-function mutation; tonic inhibitory current; cerebellar granule cells.

Introduction

Tonic inhibitory signaling is one of the key modulatory mechanisms of neural cell crosstalk and, as a consequence, neural network functioning in the brain (Farrant & Nusser, 2005). This form of signalling is commonly mediated by extrasynaptic receptors with a high affinity to neurotransmitter ejected to extracellular space due to synaptic spillover (Eulenburg & Gomeza, 2010). Despite active research over the past decades, our understanding of tonic inhibitory signaling mechanisms is still far from excellence. To date, the vast majority of studies examining the mechanisms of tonic inhibition have concentrated on that mediated by GABA$_A$ receptors (GABA$_A$Rs) (Mtchedlishvili & Kapur, 2006; Mann & Mody, 2009; Clarkson *et al.*, 2010). In contrast, much less attention has been paid to glycine receptors (GlyRs) which are also expressed extrasynaptically, and can generate lasting inhibitory tone (Xu & Gong, 2010; Salling & Harrison, 2014).

Cerebellar granule cells (CGCs) make a favorable model system to address the role of inhibitory conductance in information processing. CGCs are electrically compact, which allows high-resolution patch-clamp and makes them sensitive to small fluctuations of electrical conductance (Virginio & Cherubini, 1997), undergo strong inhibition (Rossi *et al.*, 2003; Chadderton *et al.*, 2004), and form the continuous input layer which shapes information flow through cerebellar cortex (Hamann *et al.*, 2002; Chadderton *et al.*, 2004).

Concentration values for glycine (Gly) in extracellular space of cerebellar tissue display quite a noticeable difference when reported by different research groups: 8.6±2 μM (Tossman *et al.*, 1986), 18±9 μM (Matsui *et al.*, 1995), 27±12 μM (Hashimoto *et al.*, 1995). Despite these differences, this makes the cerebellum a part of brain with one of the highest extracellular concentration of Gly (Tossman *et al.*, 1986), thus suggesting an important role of glycinergic signalling in cerebellar function.

In the cerebellum, the highest density of GlyRs at cell surfaces was demonstrated for Purkinje cells and interneurons of the molecular layer, with low, but detectable, immune signal in all other areas (van den Pol & Gorcs, 1988; Sassoè-Pognetto *et al.*, 2000). When studied using molecular biology methods, GlyRs have been also found in CGCs, being localized at cell somata rather than within synaptic densities (van den Pol & Gorcs, 1988). Further electrophysiological studies have revealed fully functional GlyRs in membrane patches excised from CGC somata (Kaneda *et al.*, 1995; Virginio & Cherubini, 1997), but no

GlyR-mediated signaling in CGC synapses (Kaneda *et al.*, 1995). These data imply that the GlyRs of CGC have been exclusively (or at least to a major extent) localized to extrasynaptic cell surface, thus enabling research of the tonic GlyR-mediated inhibition without "contaminating" signaling from synaptic glycine-ergic inhibitory transmission.

Inhibitory GlyRs are pentameric Cl^- channels; functional GlyR can be homomeric, i.e. consist of five α subunits ($\alpha1$-$\alpha4$ subtypes), or heteromeric with $3\alpha+2\beta$ composition (Langosch *et al.*, 1988). The latter composition type is most typical for acute neural tissue. The T258F point mutation in the $\alpha1$ subunit is a gain-of-function mutation which was shown to increase affinity to glycine (Gly) in both homomeric and heteromeric GlyRs (Steinbach *et al.*, 2000; Shan *et al.*, 2001). This makes T258F $\alpha1$-containing GlyRs of various subunit composition a perspective object, allowing the study of tonic inhibitory conductance, as they can be activated by relatively low concentrations of endogenous ligands characteristic for extrasynaptic space. However, following initial interest, studies of T258F GlyR have been paused for more than fifteen years, thus its pharmacology in respect to ligands other than Gly, its impact on inhibitory response kinetics, not to mention its functional role in inter-neuronal signalling, remain unknown.

Hyperekplexia, or startle disease, is a neuromotor disorder caused by deficits in glycinergic brain signaling and, at least in some cases, associated with cerebellar vermis (Leaton & Supple, 1986; Lopiano *et al.*, 1990). The gain-of-function mutations of the GlyR $\alpha1$ subunit were repeatedly shown to cause hyperekplexia (Chung *et al.*, 2010; Bode *et al.*, 2013) via the ablation of $\alpha1\beta$ glycinergic synapses (Zhang *et al.*, 2016). This is, however, unlikely the case for the cerebellar effects associated with CGCs due to the absence (or extreme scarcity) of glycinergic synaptic connections at these cells. Thus the dissection of the effects of GlyRs carrying gain-of-function mutation in CGCs may provide a key to cellular and molecular hyperekplexia mechanisms which are currently not in the focus of neuroscience research.

Apart from Gly (Billups & Attwell, 2003), another endogenous GlyR ligand released in cerebellum upon depolarization is β-alanine (Ala) (Saransaari & Oja, 1993; Koga *et al.*, 2002). Despite being much less potent than Gly, when acting at GlyR (Pan & Slaughter, 1995), endogenous Ala has been shown to generate tonic GlyR-mediated current in living neural tissue (Mori *et al.*, 2002).

Therefore, in this study we dissect the role in neuronal signaling and functional properties of T258F GlyR in comparison with wild-type (WT) receptor after activation by Gly and Ala. We set out to go from volatility of single-channel electrical conductance to the impact of tonic GlyR-mediated current on cerebellar neural network functioning, connecting these points via the modulation of inhibitory response kinetics and the regulation of action potential generation.

Materials and methods

Ethical approvals

All experiments on animals were conducted in strict accordance with UK Animals (Scientific Procedures) Act 1986 Schedule 1 and the Australian National University ethical committee regulations.

HEK cell cultures

Human embryo kidney 293 cells (HEK-293) were grown in 10-cm tissue culture dishes coated with a mixture of rat tail Type I collagen at 0.5 mg/ml and poly-D-lysine at 0.1 mg/ml at 37°C, 5% CO_2, in a saturated water atmosphere, cultivated in minimum essential medium, supplemented with 10% fetal calf serum, 100 IU penicillin, 100 μg/l streptomycin, and passaged twice weekly.

Since expression of α2 GlyR subunit in CGCs sharply decreases during the first three weeks of postnatal development to the level characteristic for adult organism, whereas expression of α1 and β subunits increases over the same period (Lynch, 2009), we transfected HEK cells and cultured CGCs with α1 subunit DNA to mimic a receptor composition characteristic for 25-30 days old animals which were used as a source of acute cerebellar tissue.

HEK-293 cells were transfected by calcium phosphate - DNA coprecipitation protocol (Chen & Okayama, 1987) with cDNA coding for the α1 glycine receptor subunit (T258F or WT) and β subunit (WT) and for the green fluorescent protein as a marker. When co-transfecting the GlyR α1 and β subunits, their respective cDNAs were combined in a ratio of 1:10 (Pribilla *et al.*, 1992). Recordings were carried out 24–72 hours after transfection. The perfusion solution contained (in mM): 140 NaCl, 4 KCl, 2 $CaCl_2$, 2 $MgCl_2$, 10 HEPES, 10

glucose; pH was adjusted to 7.4 with NaOH, osmolarity 300–310 mOsm. Recording pipettes were made from borosilicate glass capillaries, 1.5mm OD, 0.86 mm ID. Pipettes used for whole-cell recordings had resistances 2-3 MΩ, for patch recordings 4-5 MΩ. Both pipettes for patch- and whole-cell recordings contained (in mM): 145 CsCl, 2 CaCl$_2$, 2 MgCl$_2$, 10 HEPES, 10 EGTA, with the pH adjusted to 7.4 with CsOH and osmolarity adjusted to 300–310 mOsm. Drug application was performed using 8-channels set of U-tubes, ligands were dissolved in perfusion solution. The flow pipes had an individual tip diameter of approximately 40 μm and were arranged in a square pattern. For the rapid solution application experiment we adapted a RASE protocol (Sylantyev & Rusakov, 2013) allowing application of series of different solutions at the same patch with up to 150-200 μs time resolution. Briefly, patches were exposed to the solution flow from θ-glass pipette mounted on piezo-actuator, with up to three different solutions exchanged in each application pipette channel; solution application on patch pipette tip was performed by switches of piezo-actuator driven by DSA-2 constant-voltage stimulus isolator (Digitimer Ltd). Experiments were performed at 33-35ºC with holding potential of -60 or -70 mV. Data acquisition and online analysis were performed with AxoGraph 4.0 and pClamp/Clampfit 10x software. Analysis of current transients activated by +5 mV voltage steps in voltage-clamp mode gave 11.17±0.2 pS as a value of HEK cell membrane capacitance (n=217), which reproduces earlier reports (Avila *et al.*, 2004; Fischmeister & Hartzell, 2005).

Cerebellar acute slices

C57Bl-6J mice were bred in the institutional animal house, grown on a Rat and Mouse Breeding Diet (Special Diet Services, Witham, UK) and water *ad libitum*, and maintained at 12–12-h light-dark cycle. Animals were sacrificed for slices in the first half of light period of the L/D cycle. To kill animals, we used an overdose of isoflurane according to the United Kingdom Animals (Scientific Procedures) Act of 1986. After decapitation with guillotine, brains were rapidly removed and dissected, and cerebellums were sliced.

250 μm parasagittal slices were cut from the cerebellar vermis of 25-30 days old mice with a Leica VT1200S vibratome and incubated for one hour in a solution containing (in mM): 124 NaCl, 3 KCl, 1 CaCl$_2$, 3 MgCl$_2$, 26 NaHCO$_3$, 1.25 NaH$_2$PO$_4$, 10 D-glucose, and bubbled with 95:5 O$_2$/CO$_2$, pH 7.4. After incubation slices were transferred to a recording chamber continuously superfused with an external solution. The external solution composition differed from incubation solution in containing 2 mM CaCl$_2$ and 2 mM MgCl$_2$. GlyR-delivered

conductance was isolated with a ligands cocktail containing 50 μM APV, 20 μM NBQX, 50 nM CGP-55845, 200 μM S-MCPG, 10 μM MDL-72222, and 1 mM pentylenetetrazole (PTZ) as $GABA_A$-receptor antagonist which has no or low impact on GlyR effects (Corda *et al.*, 1991; Blednov *et al.*, 2012), which is not the case for other commonly used antagonists of $GABA_A$-receptor (Wang & Slaughter, 2005).

The mossy fiber – granule cell pathway morphology is identical for the whole cerebellum; thus any part of cerebellar granule cell layer with adjacent white matter can be used as a representative experimental object. However, to preserve the pathway intact in biplanar slice, vermis rather than cerebellar hemispheres should be used: otherwise, due to bends of lobules in three dimensions, biplanar slice brakes into small separate pieces (Garthwaite & Batchelor, 1996). Therefore, in our preparation we used slices of cerebellar vermis, where high-frequency stimulation was delivered to mossy fiber axons by DSA-2 stimulus isolator via bipolar tungsten electrode placed in the cerebellar white matter near the gyrus crest to stimulate mossy fibers entering the granule cells layer (Garthwaite & Batchelor, 1996). To stimulate a single mossy fiber, we used a θ-glass electrode pulled to ~5 μm tip diameter, filled with perfusion solution, with wires in both channels connected to the stimulus isolator.

In all experiments on CGCs (in acute tissue or in culture) the intracellular pipette solution for voltage-clamp recordings contained (mM): 117.5 Cs-gluconate, 17.5 CsCl, 10 KOH-HEPES, 10 BAPTA, 8 NaCl, 5 QX-314, 2 Mg-ATP, 0.3 GTP; for current-clamp recordings: 126 K-gluconate, 4 NaCl, 5 HEPES, 15 glucose, 1 MgSO4*7H$_2$O, 2 BAPTA, 3 Mg-ATP; (pH 7.2, 295 mOsm in both cases); pipette resistance was 7-9 MΩ; recordings were performed at 33-35ºC using Multiclamp-700B amplifier with -60 or -70 mV holding current (for voltage-clamp recordings); signals were pre-filtered and digitized at 10 kHz.

Cultured granule cells

Primary cultures of cerebellar granule neurons were prepared from postnatal days 25–27 mice. Animals were sacrificed as it was described above. The cerebellums were then removed, dissociated with 0.25 mg/ml trypsin, and plated in 35 mm Nunc dishes at a density of 1.5×104 cells/ml on glass coverslips coated with poly-D-lysine (10 μg/ml). The cells were cultured in basal Eagle's medium supplemented with 10% bovine calf serum, 2 mM glutamine, and 100 μg/ml gentamycin at 37°C in 5% CO2. At days in vitro (DIV) 5 the medium was replaced with 5 mM K^+ medium supplemented with 5 mg/ml glucose, 0.1

mg/ml transferrin, 0.025 mg/ml insulin, 2 mM glutamine, 20 μg/ml gentamycin and 10 μM cytosine arabinofuranoside, as previously described (Losi et al., 2002), to facilitate formation of synaptic network. Cultured neurons were transfected at DIV 7 with WT α1 or T258F α1 and green fluorescent protein (GFP) plasmids with a calcium phosphate protocol. Recordings were performed starting from DIV 10. The perfusion solution contained the following (in mM): 119 NaCl, 2.5 KCl, 1.3 Na_2SO_4, 2.5 $CaCl_2$, 26.2 $NaHCO_3$, 1 NaH_2PO_4, 22 glucose and was continuously gassed with 95% O_2/5% CO_2, pH 7.35, osmolarity 290–298 mOsm.

To assess modulation of synaptic efficacy in polysynaptic signalling pathways we used experimental approach tested on cell cultures earlier (Bi & Poo, 1999). Briefly, evoked postsynaptic currents (EPSCs) were recorded from the neuron in a network of 20-30 cells (cut from surrounding cell culture by blunt electrode) after current injection applied to another patched neuron nearby. For the sake of clarity, we isolated segments of neuronal networks containing only one GFP-fluorescent cell, which was recorded when transfection with human WT or T258F α1 subunit was studied; or no GFP-fluorescent cells under control. Perfusion solution in this experiment did not contain neural receptor antagonists. Each EPSC component propagated by recorded neuron was interpreted as a signal delivered through separate polysynaptic pathway with a specific transmission delay. To quantify the impact of GlyRs on synaptic efficacy, we measured probability of EPSC components occurrence (P) in control and after series of paired stimuli. To allow registration of both increase and decrease of P, in the beginning of experiment stimulation was adjusted to generate P in an interval 25%<P<75%. If under control conditions EPSC component had P out of this interval, the component was not used in further statistical calculations. Analysis of current transients activated by +5 mV voltage steps in voltage-clamp mode gave 2.93±0.11 pS as a value of CGC membrane capacitance (n=186) which resembles earlier observations (D'Angelo *et al.*, 1995; Hevers & Lüddens, 2002).

Data analysis

Analysis of the macroscopic currents. Continuous application of GlyR ligands evoked macroscopic responses, where "stable" response was determined as a difference between average value of baseline (2-3 s interval before ligand(s) application) and stable current generated at 5-10 s interval after stabilization of recording current after ligand(s) application.

Analysis of concentration-response relationships. Concentration-response curve fitting for changes of response amplitude (A_{GlyR}) was performed with Hill equation

$$A_{GlyR} = \frac{C^{n_h}}{EC_{50} + C^{n_h}}$$

for agonists, and

$$A_{GlyR} = 1 - \frac{C^{n_h}}{EC_{50} + C^{n_h}}$$

for strychnine, where C is a ligand concentration, EC_{50} – concentration which causes half-maximum effect, n_h – Hill's coefficient.

Analysis of phasic responses. Decay profiles of phasic responses were fitted with an exponential function

$$\Delta I = -ae^{\frac{-t}{\tau}}$$

where ΔI is a difference between current recorded at baseline and at time t, e – the Euler's constant, a – fitting constant, τ – decay time constant.

Analysis of the single-channel recordings. Application of GlyR agonists at outside-out patches evoked single-channel openings to several conductance levels. Therefore, to calculate and visualize average GlyR conductance characteristic, we constructed all-points histograms and fitted them with a multi-Gaussian function:

$$F = \frac{p_1 e^{-\frac{(n-m_1)^2}{2\sigma_1^2}}}{\sigma_1 \sqrt{2\pi}} + \frac{p_2 e^{-\frac{(n-m_2)^2}{2\sigma_2^2}}}{\sigma_2 \sqrt{2\pi}} + ... + \frac{p_k e^{-\frac{(n-m_k)^2}{2\sigma_k^2}}}{\sigma_k \sqrt{2\pi}} \, ,$$

where k is a number of peaks at a histogram, m_1, m_2 … m_k are the mode values of Gaussians, σ_1, σ_2 … σ_k are the standard deviations of corresponding modes, n is the value of electrical current, p_1, p_2 … p_k are the fitting constants, e is the Euler's constant. The general algorithm of multi-Gaussian histogram construction, fitting and interpretation was adapted from the works of Bennett and Kearns (Bennett & Kearns, 2000) and Traynelis and Jaramillo (Traynelis & Jaramillo, 1998).

To quantify input of each conductance level into overall charge transfer, we first obtained a value of the overall charge transfer as a sum of dot values (ΣI_o) in recorded traces for which is true the inequality $I_o \leq I_{m1} + 2*I_{\sigma1}$, where I_o is a (negative) current recorded when GlyR is in an open state, I_{m1} – (negative) current which corresponds to the smallest conductance peak of multi-Gaussian fitting function, $I_{\sigma1}$ – (positive) current value which corresponds to the value of standard deviation of the smallest conductance peak. Next, we obtained charge transfer for each conductance level as a sum of dot values (ΣI_c) in recording trace for which is true the inequality $I_c + 2*I_{\sigma c} \geq I_c \geq I_c - 2*I_{\sigma c}$, where I_c – current which corresponds to the Gaussian peak at a certain conductance level, $I_{\sigma c}$ – current value which corresponds to the value of standard deviation of this Gaussian peak. Part of each conductance level in an overall charge transfer was then calculated as $\Sigma I_c / \Sigma I_o * 100\%$. Single channel openings to certain conductance were selected automatically by the threshold-detection algorithm of Clampfit software with a minimum event time length of 0.2 ms.

For the semi-quantitative assessment of amount of GlyR agonists released from cerebellar tissue in response to high-frequency stimulation in a sniffer patch experiment we used an open time fraction of single-channel patch recording. This was calculated as a ratio t_o/t_c, where t_o is a full time of a given recording when GlyR(s) in a patch where in open state and t_c is a time when GlyR(s) where in closed state.

Analysis of tonic currents. For analysis of tonic whole-cell currents, mean values of holding current were averaged at 30 s intervals. The shift of the tonic current was calculated as the difference between the holding current values (ΔI_{hold}) measured at stable baseline intervals before and after the application of 1 μM strychnine.

CGP-55845, S-MCPG, strychnine, MDL-72222, picrotoxin, tetrodotoxin, bicuculline and pentylenetetrazole were purchased from Tocris Bioscience. APV, NBQX and QX-314 were purchased from Alomone Labs. Cell culture mediums, trypsin, bovine calf serum and antibiotics were purchased from Invitrogen. All other chemicals were purchased from Sigma-Aldrich. The WTα1 GlyR plasmid and GFP plasmid were kindly donated by Prof. Peter Schofield from the Garvan Institute, Sydney; T258Fα1 plasmid was kindly donated by Prof. Joseph Lynch from the University of Queensland, Brisbane. The α2 and β GlyR plasmids were purchased from OriGene.

All data are shown as Mean±S.E.M. Two-way and one-way analysis of variance (ANOVA) with Tukey post-hoc test, and Student's paired and unpaired t-test were used for statistical calculations as indicated. Nonlinear fitting and related statistical calculations were performed with Wolfram Mathematica 11 software package.

Results

Effect of T258F mutation and GlyR subunit composition on affinity to ligands

Initially, dose-response dependencies for GlyR ligands at T258F and WT GlyRs were tested, with EC_{50} (or IC_{50} for "strychnine vs. agonist") and Hill coefficient (n_h) as quantitative readouts (refer to Tables 1 and 2 for numerical values).

Increasing concentrations of Gly and Ala were first applied to HEK-293 cells expressing homomeric ($\alpha 1$) and heteromeric ($\alpha 1\beta$) GlyRs, and two-way ANOVA with a Tukey post-hoc test was used for the data analysis. When we measured the effect on peak current, obtained values had high variability and thus were hardly interpretable (Table 1). The possible explanation for this phenomenon is an initial turbulence in applied solution that activates neighboring cells, which then transfer electrical signal to the recorded cell. This transfer is enabled by gap junctions (connect >90% of abutting HEK cells) and tunneling nanotubes (connect ~50% of distant HEK cells) (Wang *et al.*, 2010). Additionally, in some recordings, maximum current amplitude was observed for stabilized (equilibrated) effect (Fig. 1D). Hence, for the whole-cell recordings we took measurements at a time interval where the effect was already equilibrated (Fig. 1A-D). Here and in further experiments we used for ANOVA purposes an agonist (Gly or Ala) as the independent factor1 and a GlyR subunit composition as the independent factor2.

We found, that EC_{50} of Ala was significantly higher than for Gly, but no significant difference between agonists was observed for generated n_h. GlyR subunit composition also exerted a significant impact on EC_{50} values: presence of β subunit or T258F $\alpha 1$ subunit lowered an agonist's EC_{50}; however, only presence of T258F $\alpha 1$ subunit, but not β subunit, made a significant impact on n_h (see Table 1, Fig. 1A, B, I, J).

Two-way ANOVA on values of EC_{50}. Factor1: $F_{1,41}=16.31$, $P=2*10^{-4}$; Factor2: $F_{3,41}=10.37$, $P=3.3*10^{-5}$, Tukey test: $P>0.05$ for T258F$\alpha 1$ vs. T258F$\alpha 1\beta$; for factor1×factor2: $F_{3,41}=3.18$,

P=0.034. Two-way ANOVA on values of n_h. Factor1: $F_{1,41}$=2.78, P=0.103; Factor2: $F_{3,41}$=6.12, P=0.0015, Tukey test: P>0.05 for WTα1 vs. WTα1β and for T258Fα1 vs. T258Fα1β; factor1×factor2: $F_{3,41}$=2.42, P=0.08.

Next, we studied the strychnine (Str) effects on WT and T258F GlyRs against the previously found EC_{50} of agonists. Here presence of the T258Fα1 subunit significantly increased the IC_{50} values of Str, whereas presence of β subunit did not make a significant impact; no significant difference between Gly and Ala in terms of counteracting Str effect was found. Neither subunit composition, nor type of agonist induced a significant bias of n_h (Table 1, Fig. 1C, D, K, L).

Two-way ANOVA on IC_{50} data: factor1, $F_{1,37}$=2.56, P=0.118; factor2, $F_{3,37}$=7.92, P=3.3*10^{-4}, Tukey test: P>0.05 for WTα1 vs. WTα1β and for T258Fα1 vs. T258Fα1β; factor1×factor2: $F_{3,37}$=2.09, P=0.118. Two-way ANOVA on n_h values: P>0.1 for both factors.

Whole-cell recordings from HEK cells confirmed a pharmacological profile of GlyRs expressed from our plasmids. As a next step, we set out to test whether pharmacological properties of expressed GlyRs are similar in different cultured cell types (HEK and CGC) and in CGCs of living tissue. Our working hypothesis was as follows: α1 subunits, being expressed in CGCs, mainly generate heteromeric GlyRs with β subunits naturally expressed in this cell type. Therefore, the pharmacological profile of GlyRs in CGCs transfected with WTα1 and T258Fα1 plasmids should be similar to that of WTα1β- and T258Fα1β- transfected HEK cells, respectively. As a consequence, pharmacological profile of CGCs in living tissue should be similar to WTα1β-transfected HEK cells.

To obtain more controlled experimental environment, we first tried to apply Gly and Gly+Str at outside-out membrane patches instead of whole cells. The vast majority of outside-out patches excised from both cultured CGCs and CGCs of cerebellar brain slices (8 out of 11 tried) after application of Gly displayed single-channel openings rather than poly-receptor response of a kind as was observed in a whole-cell mode. However, when we repeated the experiment with nucleated patches, poly-receptor response was generated in all trials (see example traces at Fig. 1E-H). Values of Gly EC_{50}, Str IC_{50} and n_h obtained for peak current in nucleated patches were similar to that of HEK cells transfected with WTα1β, cultured CGCs transfected with WTα1, CGCs from living tissue, and WTα1β-transfected HEK cells recorded in whole-cell mode: P>0.3 for all comparisons, n=10-13, Student's t-test.

Another set of similar readouts was obtained for nucleated patches from T258Fα1β-transfected HEK cells, T258Fα1-transfected CGCs and T258Fα1β-transfected HEK cells in whole-cell mode: P>0.2 for all comparisons, n=10-12, Student's t-test; see Tables 1 and 2 for numerical data. These results have supported our working hypothesis and thus confirmed similar pharmacological profiles of GlyRs expressed in cell cultures and in living tissue.

Effect of T258F mutation and GlyR subunit composition on receptor conductance

As a next step, we tested the mutation effect on GlyR single-channel electrical conductance in outside-out patches excised from HEK cells (Fig. 2; see Table 3 for numerical data). Here we applied the lowest agonist concentration which exerted a significant effect in whole-cell experiment on the corresponding type of GlyR (Fig. 1). We found that all-point histograms for homomeric receptors are best-fitted with three Gaussians, indicating three main conductance states, whereas the presence of a β subunit reduced the number of conductance states to two (Fig. 2C, D). For all GlyR subunit compositions, the highest conductance state delivered >85% of the overall charge transfer (Table 3). Therefore, to assess the influence of agonists and GlyR subunit composition on GlyR conductance, we analyzed data on the openings to highest conductance. We found, that presence of both T258F α1 subunit and β subunit lowers the highest conductance level, whereas no significant difference in this GlyR characteristic was observed when Ala or Gly has been applied.

Two-way ANOVA output: factor1, $F_{1,44}=1.37$, P=0.25; factor2, $F_{3,44}=5.12$, P=0.004, Tukey test: P>0.05 for WTα1β vs. T258Fα1β; factor1×factor2: $F_{3,44}=2.61$, P=0.063.

To compare single-channel characteristics of GlyRs expressed in HEK cells to those expressed in CGCs, we repeated the experiment on outside-out patches excised from cultured CGCs transfected with WTα1 and T258Fα1 plasmids, and from CGCs of living tissue (Table 4). In all three experiments on CGCs single-channel GlyR conductance had no significant difference from values obtained when WTα1β and T258Fα1β receptors were expressed in HEK cells: P>0.2 for all comparisons, n=12, Student's t-test (see Table 3 and 4).

GlyR subunit composition shapes response kinetics

For deeper analysis of GlyR functional properties, we next studied the decay kinetics of response evoked by brief (~200 μs) applications of 50 μM Gly and 500 μM Ala in membrane patches carrying GlyRs of different types. This experiment again demonstrated the significant

impact of both agonist species and GlyR subunit composition on the response kinetics (Fig. 3). To quantify this impact, we used values of decay time constant (τ) obtained with a nonlinear fitting of response decay profiles. Responses generated by Gly displayed significantly slower decay (higher decay τ) than responses generated by Ala; presence of β subunit, but not T258Fα1 subunit made decay faster, i.e. lowered τ values.

Two-way ANOVA results on τ values. For factor1: $F_{1,40}=205$, $P=2.5*10^{-17}$; for factor2: $F_{3,40}=24.6$, $P=3.5*10^{-9}$, Tukey test: $P>0.05$ for WTα1 vs. T258Fα1; for factor1×factor2: $F_{3,40}=9.6$, $P=6.6*10^{-5}$.

To test whether results obtained for GlyRs expressed in HEK cells are applicable to CGCs, we repeated this experimental protocol at nucleated patches excised from cultured CGCs under control (no additional transfection), CGCs transfected with WTα1 plasmid, and CGCs transfected with T258F plasmid, applying 50 μM Gly (Fig. 3E, F). We found, that transfection with T258Fα1, but not with WTα1, slowers significantly response decay kinetics when compared to control. For T258Fα1 vs. control: $P=0.004$, $n=12$; for WTα1 vs. control: $P=0.39$, $n=12$, Student's t-test. This result reproduces an observation for HEK cells transfected with T258Fα1+β and WTα1+β (Fig. 3A, B). Hence it is in line with the presumption that, being transfected with WTα1, CGC generates heteromeric WTα1β GlyRs, similar to native GlyRs of CGC and to those generated in HEK cell transfected with WTα1+β plasmids. In turn, transfection of CGC with T258Fα1 results in a mixture of heteromeric T258Fα1β and WTα1β GlyRs.

GlyR sensitivity to GABA$_A$R open-channel blockers

Single-receptor recordings revealed two different modes of the main conductance state: ~100-110 pS for HEK cells transfected with WTα1 and T258Fα1 and ~50-60 pS for WTα1β- and T258Fα1β-transfected HEK cells, WTα1- and T258Fα1-transfected CGCs, and CGCs of living tissue (Tables 3 and 4). This pattern suggests that (i) α1 subunits expressed from transfected DNA form heteromeric GlyRs with wild-type β subunits when they are present in a given cell, and (ii) properties of these receptors a similar to those in CGCs of acute tissue.

To further confirm this finding and to test whether GABA$_A$R open-channel blockers such as picrotoxin (PTX) and pentylenetetrazole (PTZ) do not affect heteromeric GlyR functioning in

our preparation, we performed an additional solution exchange experiment on nucleated patches. In this experiment each patch underwent application of 10 μM Gly and then 10 μM Gly + 10 μM PTX, or 10 μM Gly + 1 mM PTZ (Fig. 4). PTX, being applied at patches from WTα1-transfected HEK cells, lowered the response amplitude to 0.42±0.16 of control: P=0.022, n=6, Student's paired t-test. For all other sets of plasmids expressed in both HEK and CGCs, and for nucleated patches from CGCs of living tissue, PTX and PTZ did not display a significant effect: P>0.3, n=6 for all cases, Student's paired t-test (Fig. 4D). PTX, displaying a significant effect exclusively at homomeric WTα1 receptors, has confirmed earlier observations (Pribilla *et al.*, 1992; Shan *et al.*, 2001). Hence, we received an additional confirmation of heteromeric composition of GlyRs in all cell types where β GlyR subunit is expressed. In turn, 1 mM PTZ did not exert a significant effect on any GlyR type (in accord with earlier studies, see (Corda *et al.*, 1991)), thus enabling us to use it for silencing of GABA$_A$Rs in further experiments on living tissue with presumable GABA spillover.

As an additional control on subunit composition of GlyRs in CGCs, we tested the antagonist effect of bicuculline (BIC) on α1β and α2β GlyRs expressed in HEK cells and on GlyRs from CGCs of acute tissue. 1 mM BIC, when applied against 60 μM of Gly, was shown to block in full conductance generated by α2β GlyRs, but not by α1β GlyRs (Li & Slaughter, 2007). We repeated this experimental protocol to find, that 1 mM BIC indeed fully suppressed the effect of α2β GlyRs in HEK cells (response amplitude 0.045±0.007 of control), but not α1β GlyRs in HEK cells and GlyRs from CGC of acute tissue: 0.392±0.096 and 0.43±0.089 for HEK cells and CGCs, respectively (Fig. 4C and E). This result confirmed that α1-containing GlyRs generate at least a significant part of GlyR effect in CGCs of 25-30 days old C57Bl-6J mice and provided rationale of the α1 overexpression experiments.

GlyR input into tonic conductance in living neural tissue

Previous experiments allowed us to assess the influence of mutant GlyR subunits on single-channel properties, and on poly-receptor response parameters in an artificial expression system (HEK cells) as well as in cultured CGCs and CGCs from acute slices. Therefore, in the next stage of the research we decided to test the GlyR impact on inter-neuronal signaling in living cerebellar tissue.

As a first step, we clarified whether GlyR conductance has a significant input into neural tonic signaling in cerebellar vermis. To achieve this, we performed a continuous whole-cell

recording from CGCs in vermis slices (Fig. 5). To isolate GlyR activity we added a cocktail of ligands (including PTZ), which blocked all other receptors (see "*Cerebellar acute slices*" section of Methods for more details). GlyR response-isolating ligands fully suppressed spontaneous activity in CGCs. However, subsequent applications of 1 μM strychnine did not induce any significant effect, shifting the holding current for 1.57$\pm$0.84 pA; the significance of the difference from zero being: P=0.103, n=8, Student's t-test (Fig. 5A, D). We therefore repeated the experimental protocol, adding high-frequency stimulation (HFS): 8 bursts of 10 impulses at 100 Hz delivered to mossy fibers (D'Angelo *et al.*, 1999) 10 minutes before drug application. After HFS, application of strychnine following GlyR-isolating ligands revealed the presence of GlyR-mediated tonic conductance of 5.38$\pm$0.82 pA, thus proving the presence of functional tonically-active GlyRs; the significance of the difference from zero was: P=3.1*10^{-4}, n=8, Student's paired t-test (Fig. 5A, D).

We next asked, what is the mechanism revealing GlyR-mediated tonic conductance after HFS. The simplest explanation is that HFS upregulates the synaptic vesicular release which results in neurotransmitter spillover and, as a consequence, results in an increase of neurotransmitters (in particular Gly) concentration in extracellular space. To test this hypothesis, we repeated the experiment without HFS, but with Ca^{2+} concentration elevated to 4 mM which should promote vesicle release. Indeed, under these conditions we observed a significant GlyR-mediated tonic current, similar to that after HFS: 6.02$\pm$0.73 pA; the significance of the difference from zero: P=1.8*10^{-4}, n=7, Student's paired t-test (Fig. 5A, D).

Additionally, to explore whether our GlyR response-isolating cocktail fully inhibits all activity of GABA$_A$Rs, we repeated a HFS experiment, but with application of 50 μM PTX after PTZ-containing cocktail (Fig. 5B). Under these conditions, we found no significant effect of PTX which induced an outward shift of holding current for 0.67$\pm$0.42 pA (P=0.53, n=6, Student's paired t-test), but still a significant effect of strychnine added after PTX: 5.42$\pm$0.54 pA, P=4.2*10^{-4}, n=6, Student's paired t-test (Fig. 5B, E). Next, to clarify whether the impact of strychnine on holding current is not due to its side effect on GABA$_A$Rs, we performed a continuous recording experiment without HFS, when GlyR response-isolating cocktail was not applied before strychnine, and PTX was applied after strychnine (Fig. 5C). In this experiment strychnine did not display a significant impact on holding current (difference from control 1.11$\pm$0.32 pA, P=0.66, n=6, Student's paired t-test), whereas PTX

still induced its significant outward shift (difference from strychnine 10.3±0.97 pA, P=0.0002, n=6, Student's paired t-test) - see Fig. 5F.

Release of GlyR endogenous ligands in cerebellar tissue due to HFS

Next, to test directly whether cerebellar tissue releases an additional amount of GlyR agonists in a course of HFS, we combined a HFS stimulation with a sniffer patch technique (Fig. 6). To do this, we pulled an outside-out patch from CGC, and performed a control recording of GlyR openings at a distance of 5 μm from slice surface. Then we repeated a recording at 300 μm above the slice. Next, we lowered the patch pipette back to 5-6 μm distance and initiated HFS stimulation protocol; after that we again elevated the patch pipette to 300 μm distance (Fig. 6A). For quantitative assessment of HFS effect on neurotransmitters' release we calculated values of an open-time fraction which integrates single-channel open time and opening frequency (Fig. 6B). The value of GlyR open time fraction recorded at 5 μm distance under HFS was 2.06±0.26 times higher than that obtained under control conditions at the same distance (P=0.009, n=6, Student's paired t-test). In contrast, the open time fraction was significantly lowered at a 300 μm distance when compared to that obtained at 5 μm under control: to 0.082±0.031 at 300 μm under control conditions and to 0.087±0.032 under HFS; P<0.0001, n=6 for both cases, Student's paired t-test.

GlyRs of CGCs modulate action potential generation

An experiment on acute tissue has proved the presence of tonically active GlyRs in CGCs. Hence, we next asked if extrasynaptic GlyRs of CGC modify neuronal signalling generation, and if so, how can this role be modified by the gain-of-function mutation? To clarify this, we performed experiments on cultured CGCs transfected with T258Fα1 subunit, and WTα1 subunit as a positive control ensuring that experimental results observed in T258Fα1-expressing culture are not the side effects of the transfection procedure. The abundance of native β GlyR subunits in CGCs (AIBS) ensured the formation of heteromeric receptors in the transfected cells.

First, we studied modulatory input of tonically active GlyRs into the action potential generation. To do this, we compared the summation profile of evoked post-synaptic potentials (EPSPs) during trains of five stimuli evoked by the field 50 Hz stimulation. The

stimuli strength was adjusted so that, under control conditions where no GlyR ligands added, the stimulation train induced 1-3 APs (Fig. 7A-C). After the control recording series (10 traces) stimulation protocol was repeated on the same cell with low concentrations of GlyR agonist (10 μM Gly or 50 μM Ala) and then with high concentrations of agonist (50 μM Gly or 500 μM Ala), a total of ten individual traces for each mode. The average number of APs per trace was then used for quantification of the agonist effect. The experiment was repeated for untransfected cells, cells transfected with WTα1, and with T258Fα1 cDNA. Both agonists displayed a similar response profile in untransfected CGCs and CGCs transfected with WTα1: only a high ligand concentrations exerted a significant downregulatory impact on AP numbers; on the contrary, in the case of CGCs transfected with T258Fα1, a significant decrease of AP number was generated after application of agonists in both concentrations (Fig. 7D-E).

Tonically active GlyRs modulate synaptic plasticity

An experiment on EPSP summation confirmed the significant input of GlyRs into AP generation machinery. However, how could this affect the synaptic plasticity and inter-neuronal crosstalk? To address the issue, we studied networks composed of several (20-30) cultured CGCs, where two polysynaptically connected cells were patched simultaneously. Current injection into one cell generated an action potential with the subsequent poly-component EPSC recorded from another cell. We interpreted each EPSC component as a signal transmission through separate pathways with a specific time lag. When the low-frequency stimulation (1 stimulus per 15 seconds) was used, the occurrence probability (P) remained stable for each EPSC component. We thus used the EPSC profile as a gauge allowing the quantitative measurement of synaptic efficacy (see the "*Cultured granule cells*" section of Methods). To examine the synaptic plasticity in the recorded network, we applied a train of 50 paired-pulse stimuli with 50 ms inter-pulse interval at 1 Hz. After that, we monitored changes in the P (decrease or increase, i.e. ΔP) of the pre-existing EPSC components. These changes were interpreted as an indicator of the remodeling of signaling pathways (Fig. 8A). At each recorded CGC, the experimental protocol was then repeated with low and high concentrations of agonists (similar to those used in the experiment on AP generation).

Unexpectedly, we found that 10 μM Gly increased significantly ΔP in untransfected cells and in cells transfected with WTα1, whereas a 50 μM concentration of Gly had a significant

downregulatory effect. On the contrary, in the cells transfected with T258Fα1, both Gly concentrations displayed a downregulatory action (Fig. 8D). The experiment with Ala did not display opposite effects for different concentrations: ΔP was decreased in all cases (Fig. 8C). To explain such a difference between the GlyR agonists, we hypothesized that the Gly-generated effects in this experiment were partially delivered through NMDA receptors (NMDARs) in parallel with GlyRs. To test this hypothesis, we repeated the experimental protocol with 2 nM of L-689,560, which is a high-affinity competitor for the Gly binding site of NMDAR (Grimwood *et al.*, 1992), in perfusate. Indeed, under these conditions, Gly displayed an effect profile similar to that of Ala: decreased ΔP under all tested concentrations (Fig. 8E). Next, we repeated this experiment without L-689,560, but with 1 μM Str in perfusion solution (Fig. 8F). Here we found, that increasing Gly concentrations elevate ΔP rather than generate bi-phasic effect as at Fig. 8D. We thus concluded, that Gly increases ΔP acting at NMDARs, and decreases ΔP acting at GlyRs.

Gly spillover modulates AP generation in CGCs of acute tissue

In the previous experiment we found that extrasynaptic GlyRs shape neural network functioning and can reverse the effect of glutamatergic excitatory input. However, it is unknown whether extrasynaptic GlyRs modulate CGCs excitation in living tissue. To clarify this, we tested GlyRs input into excitation machinery in cerebellar brain slices. Initially, we tried to reproduce a sensory excitatory input into given CGC, which was shown *in vivo* to be delivered via a single mossy fiber (Chadderton *et al.*, 2004). To achieve this, we used a θ-glass stimulation microelectrode of ~5 μM diameter. With this electrode we searched for a position in the cerebellar white matter where stimulation pulse generated EPSC(s) in the patched CGC. Once the position was found, we delivered several groups of stimuli (5 stimuli at 25 Hz, 30 s intervals between groups); each group evoked 2-5 glutamatergic EPSCs in the recorded cell, reproducing the result of *in vivo* sensory input (Chadderton *et al.*, 2004). Then we compared average response amplitudes and cumulative response amplitude histograms for evoked glutamatergic EPSCs, spontaneous EPSCs, and mini-EPSCs (after application of 1 μM tetrodotoxin, TTX): Fig. 9A, C, D. We found no significant difference in average response amplitude for these three EPSC types (one-way ANOVA: $F_{2,15}=0.47$, P=0.63) and high similarity of the cumulative response amplitude histograms (Fig. 9C). The similarity of spontaneous, evoked and mini EPSCs indicates that sensory stimulation induces bursts of

responses where each is generated by single neurotransmitter quantum, and that our stimulation protocol resembles native sensory input delivered to individual CGC.

Equipped with this knowledge, we then studied AP generation in response to sensory-like inputs. To do this, we used stimulation sets consisting of four groups, five stimuli at 25 Hz in each group, with 30 s inter-group intervals; after a first set, a 5 min interval was taken, and then similar stimulation set delivered. To quantify changes in AP-generation machinery, we used an average number of APs generated by the five-stimuli group (Fig. 9B, E, F). Under control conditions, 5 min interval with no stimulation did not significantly change an average AP number: 2.93±0.43 vs. 3.2±0.28, P=0.48, n=9, Student's paired t-test. To find out, whether AP generation is affected by Gly, we added 50 μM Gly after the first stimulation set. This significantly decreased a number of APs per stimulation group: 2.12±0.21 vs. 3.98±0.16 in the first stimulation set, P=0.00011, n=9, Student's paired t-test. To advance on this and to investigate whether cerebellar tissue can release an amount of Gly sufficient to modulate AP generation, we repeated the experiment with HFS (8 bursts of 10 impulses at 100 Hz, delivered to mossy fibers by tungsten bipolar electrode) after the first stimulation set. In this case AP number per five-stimuli group in the second stimulation set was significantly reduced: 2.83±0.4 vs. 3.53±0.36 in the first set, P=0.0014, n=9, Student's paired t-test. To test whether this effect was indeed delivered by GlyRs, we repeated the HFS experiment adding 1 μM strychnine after the first stimulation set. Strychnine made difference in AP number between the first and second stimulation sets non-significant, thus confirming GlyRs involvement: 3.47±0.21 vs. 3.27±0.28, P=0.31, n=11, Student's paired t-test.

Discussion

In this study at a first stage we have clarified the functional effects of GlyR subunits. We found that the single-point T258F mutation of α1 subunit decreases EC$_{50}$ of Gly and Ala (Fig. 1, Table 1 and 2) and slows the decay kinetics of the inhibitory response delivered via heteromeric receptors (Fig. 3). This proves that the T258F mutation increases GlyR affinity to agonists, which is in line with earlier observations (Shan *et al.*, 2001). In addition, the augmented affinity overweighs the lower conductance of T258F GlyR (compared to the WT receptor) (Fig. 2). However, on the contrary to (Shan *et al.*, 2001), in our preparation WT heteromeric (α1β) GlyRs displayed a significantly higher affinity to agonists than did WT

homomeric $\alpha 1$ GlyRs (Table 1). This resembles another study in which heteromeric GlyRs were shown to have significantly lower EC_{50} for Gly than did homomeric receptors (Mohammadi *et al.*, 2003). Overall, these facts suggest prudence when predicting GlyR effects on the basis of the receptor subunit composition. Nonetheless, experiments on HEK-293 cells have clearly shown that the introduction of the T258F$\alpha 1$ subunit increases affinity to agonists in both hetero- and homomeric GlyRs, i.e. confirmed a gain-of-function status of the T258F mutation.

Factors determining existence of multiple conductance states in GlyR and mechanisms of their implementation are the topic of long-lasting discussions. The most obvious explanation is that GlyR can open to various conductance states in response to different ligation levels: from 1 to 5 agonist molecules bound to the functional receptor (Beato *et al.*, 2004), as it was demonstrated for the closely related GABA$_A$R (Birnir *et al.*, 2001). This, however, was disproved by observations that the ratio of GlyR openings to different conductance levels is independent from the agonist concentration (Twyman & Macdonald, 1991; Beato *et al.*, 2002). Number and conductivity of GlyR conductance levels were repeatedly shown to be regulated by the receptor subunit composition (Rajendra *et al.*, 1997), where presence of β subunit eliminates high-conductance levels (Bormann *et al.*, 1993). Hence, another possibility to obtain different conductance levels in the same patch recording is a presence of GlyRs of different subunit composition in a given membrane patch. This option, however, looks quite unlikely due to observations of openings to distinct conductance levels within the same burst (Beato *et al.*, 2002). Presence of different conductance levels in recordings from outside-out patches (as at Fig. 6), where all cytoplasmic signalling chains are surely destroyed (Hamill *et al.*, 1983; Takahashi *et al.*, 1992) also questions modulation by intracellular factors as the only mechanism generating different GlyR conductance states. Therefore, available experimental facts about propagation of GlyR conductance levels suggest multiple mechanisms of their modulation. In this context, lower number of conductance levels in outside-out patches than in nucleated patches observed in our study (two vs. three) may be a result of removal of cytoplasmic factor(s) delivering partial upregulatory effect in living cell.

Residue position 258 in all types of GlyR subunits is localized within M2 domain which lines the receptor ion channel pore, making GlyR electrical conductance highly sensitive to mutations in this domain (Keramidas *et al.*, 2000; Keramidas *et al.*, 2002). Therefore, it is not surprising that the T258F mutation, i.e. replacement of small, polar and hydrophilic threonine

residue with large, non-polar and hydrophobic phenylalanine, exerts a significant downregulatory effect on GlyR electrical conductance, most possibly by obstructing the Cl^- ion passage.

The issue to be clarified before the work on GlyRs expressed in acute tissue is indeed their actual subunit composition. In situ hybridization experiments on mRNA encoding various GlyR subunits have shown that the expression level of $\alpha 1$ subunit increases, and of $\alpha 2$ subunit decreases rapidly in postnatal (after P0) tissue of spinal cord (Watanabe & Akagi, 1995). Similar experiments conducted by different research groups on CGC layer of adult rodents generated various results: strong signal for $\alpha 1$ mRNA with somatic localization (Racca *et al.*, 1998), weak signal for $\alpha 1$ mRNA (Fujita *et al.*, 1991), or no detection for both $\alpha 1$ and $\alpha 2$ subunit mRNA (Sato *et al.*, 1992). We thus tried to assess the input of $\alpha 1$-containing GlyRs into the overall GlyR signal with an alternative approach. In line with an earlier study (Li & Slaughter, 2007), we found that 1 mM BIC, being applied with 60 μM Gly, fully suppresses opening of $\alpha 2$-containing GlyRs expressed in HEK cells, but has much lower impact when $\alpha 1$-containing GlyRs were expressed. Then, being applied on GlyRs from acute cerebellar tissue, BIC approximately halved their effect, thus confirming a significant role of $\alpha 1$-GlyRs in living CGCs (Fig. 4C and E).

In our experiments on HEK cells, cultured CGCs and CGCs from acute tissue we have not observed a significant difference between heteromeric GlyRs in terms of pharmacological properties (EC_{50}, IC_{50}, Hill's coefficients) and ion channel conductance, along with similarities in percentage of overall charge transfer through given conductance state (see Tables 1-4). The impact of the T258F mutation on GlyR response decay kinetics in transfected CGCs resembles that obtained in HEK cells (Fig. 3). Moreover, PTX displayed a negligible effect on heteromeric GlyRs expressed in cultured cells and on GlyRs in membrane patches excised from CGCs of cerebellar slices (Fig. 4), thus confirming the long-established finding of PTX antagonism at $WT\alpha 1$ homomeric, but not $T258F\alpha 1$ homomeric or any type of heteromeric GlyRs (Pribilla *et al.*, 1992; Shan *et al.*, 2001). These observations suggest three main conclusions. First, physiological and pharmacological properties of GlyRs in living tissue and of heteromeric WT GlyRs expressed in different types of cultured cells are similar. Second, most GlyRs in native CGCs of 25-30 days old mice are of heteromeric composition. Third, native expression of β GlyR subunit in CGCs is high enough to make most of GlyRs heteromeric when the cell is transfected with additional amount of α-subunit

DNA; this is in accord with earlier data on much higher expression of β GlyR subunit than α subunits in postnatal CGCs (van den Pol & Gorcs, 1988; Fujita *et al.*, 1991).

The data on GlyR presence at CGC somata at different ages are to some extent contradictive. Wall and Usowicz reported the presence of GlyR-mediated currents for P12 but not for P40 animals (Wall & Usowicz, 1997); on the contrary, Sassoè-Pognetto and co-authors have found GlyR-specific immunostaining in CGCs of adult rats (Sassoè-Pognetto *et al.*, 2000). The plausible explanation of such an apparent discrepancy is that GlyR number at CGC soma decreases with age, making, at some stage, GlyR-mediated tonic current undetectable under normal conditions. Under these conditions GlyRs, however, can still be detected with immunostaining and may deliver a significant amount of tonic current after HFS which provokes neurotransmitter spillover. Therefore, to test this hypothesis and clarify a functional role of GlyRs in CGC layer, we next studied GlyRs signalling in acute cerebellar tissue.

The absence of spontaneous post-synaptic currents after the isolation of a GlyR-mediated response in our whole-cell recordings (Fig. 5A) confirms earlier reports about CGCs as being deprived of functional synaptic GlyRs, but carrying them at extrasynaptic membrane (Huck & Lux, 1987; Kaneda *et al.*, 1995; Virginio & Cherubini, 1997).

There are several possible explanations of lower amounts of GlyR-transferred current observed in CGCs than in HEK cells (see Fig. 1, 4 and 5). First, size and surface area of HEK cells are substantially larger than that of CGCs: this is illustrated by cell images (Fig. 3G) and by data on membrane capacitance (11.16 ± 0.2 pS for HEKs vs. 2.93 ± 0.11 pS for CGCs, see Methods). Second, the expression level and, as a consequence, density of GlyRs at a cell somata could be different for HEK cells and CGCs. This was confirmed by experiments finding that Gly application at membrane patches excised from HEK cells elicited macroscopic responses (Fig 3A and C), whereas the majority of outside-out patches obtained from CGCs after application of Gly displayed single-channel openings; to generate macroscopic GlyR responses in patches from CGCs the use of nucleated patches with much larger surface area was necessary (Fig. 3E). Third, as CGCs, in contrast to HEK cells, have a branched shape with several neurites (Fig. 3G), and GlyR density at dendrites increases with distance from the cell soma (Lorenzo *et al.*, 2007), in whole-cell recordings (as at Fig. 1A-D and Fig. 5) the decrease of response amplitude due to space-clamp effect should be much stronger in CGCs than in HEK cells.

GlyR-mediated tonic inhibition was shown to shape neuronal network behaviour in acute neural tissue (Flint *et al.*, 1998; Zhang *et al.*, 2008) but, to the best of our knowledge, not in the cerebellum; in our work, we could not register a significant GlyR input into tonic current under normal conditions (Fig. 5A). The plausible explanation is a low concentration of GlyR agonists in cerebellar extracellular space under stable conditions. Despite the fact that the release of Gly and Ala was repeatedly detected in native cerebellum (Koga *et al.*, 2002; Billups & Attwell, 2003) and, in particular, in cerebellar vermis (Flint *et al.*, 1981), their concentrations in the extracellular space were reported in a range of first tens of micromoles (Tossman *et al.*, 1986; Takagi *et al.*, 1993; Westergren *et al.*, 1994; Oda *et al.*, 2007), which is just above the detectable level of Gly for WT receptors found in our work, and far below this level for Ala (see Fig. 1 and Table 1). Taken together with relatively low levels of expression of GlyRs in CGCs, when compared to neighboring interneurons of cerebellar molecular layer and Purkinje cells (van den Pol & Gorcs, 1988; Racca *et al.*, 1998; Sassoè-Pognetto *et al.*, 2000), this may result in a very small amount of tonic current, undetectable with electrophysiological methods. However, HFS generated a highly significant inhibitory charge transfer via GlyRs; similar results obtained in experiment with elevated Ca^{2+} concentration supports a hypothesis concerning upregulation of neurotransmitter release as a mechanism of tonic current generation by HFS (Fig. 5D). These observations also imply that the extrasynaptic GlyRs of CGC play their functional role not on a continuous basis, but when CGC layer starts receiving high amount of excitatory inputs.

Our experimental findings on the generation of EPSP series confirmed that GlyRs input into electrical conductance exerts a substantial effect on inter-neuronal crosstalk (Fig. 7). The amount of inhibitory current transferred via GlyRs is sufficient for the control of AP generation, thus resembling the functions of tonically active GlyRs in the spinal cord (Takazawa & MacDermott, 2010).

In our subsequent experiments on the remodelling of signalling pathways, we demonstrated that the activation of GlyRs by a series of paired stimuli exerts a significant impact on the variability of synaptic transmission and synaptic strength (ΔP) – Fig. 8. Varying Gly concentrations caused an inverse change of ΔP: an increase for low concentration and a decrease for high (Fig. 8D). Since such a change of ΔP was not observed in the experiment involving Ala, when Gly was added together with L-689,560 and when GlyRs were blocked with Str (Fig. 8C, E, F), we concluded that this bi-phasic effect requires simultaneous

presence of active GlyRs and NMDARs. Therefore, we formulated a hypothesis regarding the functional role of GlyR signaling in CGCs as follows. Gly is a co-agonist that is critical for NMDAR functioning, and the elevation of incoming signaling intensity enhances Gly concentration in CGC layer (Billups & Attwell, 2003), thus ensuring NMDARs activation and AP(s) generation. However, a further increment of signaling strength activates extrasynaptic GlyRs due to the amplification of the Gly concentration. This, in turn, suppresses AP firing in CGCs and therefore discontinues (or at least limits) outgoing signaling. This hypothesis provides a plausible explanation for GlyRs relative scarcity (Sassoè-Pognetto *et al.*, 2000) and their exclusive extrasynaptic localization (Kaneda *et al.*, 1995): these are the obligatory characteristics that ensure the bi-phasic modulation of the cell signaling output, amplifying the excitatory input at low intensity, but triggering a "safety catch" which limits further excitation when input signaling rises to a certain critical level. In our experiments, T258F GlyRs, having a higher affinity to Gly, will inhibit CGCs' firing with a lower concentration of spillover neurotransmitters, which is equivalent to much weaker excitatory input.

To the best of our knowledge, there are no reports about significant Gly release (and, more importantly, spillover) in CGC synapses in response to increased excitatory input; this is in accord with the fact of the absence of GlyRs in CGC synapses (Kaneda *et al.*, 1995). Therefore, since CGCs make up >97% of neuronal population of granule cell layer (Herndon, 1964; Palay & Chan-Palay, 2012), the question about a particular mechanism of the excitation-induced Gly concentration increase in CGC layer becomes critical in a context of our hypothesis regarding Gly-based bi-phasic modulation of CGC activity. The possible source of Gly concentration increase is Bergmann glia, which is abundant in CGC layer (Herndon, 1964; Southam *et al.*, 1992) and releases significant amounts of Gly in response to cell membrane depolarization (Huang *et al.*, 2004). Such a depolarization might be due to glutamate spillover from neuronal synapses upon overexcitation, and subsequent activation of NMDA- and AMPA-receptors at Bergmann glial cells, which was shown to induce powerful cation inflow (Müller *et al.*, 1993; Dzubay & Jahr, 1999). Therefore, the critical level of excitatory input which switches Gly-mediated inhibition in CGC layer might be to large extent determined by distribution of glial Gly transporter GLYT1 (Zafra *et al.*, 1995), its activity, and sensitivity to cell membrane depolarization (Huang *et al.*, 2004).

Another important question about Gly-mediated inhibition of CGC activity is regarding its interaction and/or mutual influence with other bi-phasic modulatory systems in CGC layer,

such as glutamate-nitric oxide (NO)-cGMP pathway. In this pathway NO was shown to be a retrograde neurotransmitter which determines presynaptic ion currents, neural network excitability and long-term potentiation (LTP). In turn, NO pathway blockers inhibit neural cell excitation and LTP (D'Angelo *et al.*, 2005). It was reported earlier that when released from cerebellar neurons, NO activates soluble guanylate cyclase, thus increasing amount of cGMP in Bergmann glia (Southam *et al.*, 1992) and this way reduces Gly release (Hernandes & Troncone, 2009). This suggests the phenomenon of Gly-mediated bi-phasic regulation of CGC signaling to be an integral and tightly interconnected part of regulatory mechanisms (such as NO-cGMP pathway) that modulate cerebellar neural activity.

Our next experiment on AP generation in response to sensory-like excitatory signaling which resembles the effect of stimulation of the rodent's whisker (Chadderton *et al.*, 2004) proved a significant input of GlyRs into CGC excitation machinery in living cerebellar tissue, and provided further support to the hypothesis regarding the GlyRs functional role. We have shown, that intensive excitatory signaling activates a GlyR-mediated "safety catch" which prevents over-excitation of CGCs in response to sensory inputs (Fig. 9).

An earlier study has shown that CGCs, generating bursts of APs of limited length in response to clustered sensory-evoked signals from mossy fibers, produce patterns of activity which provide a physiological mechanism for the model of the CGC layer as a storage of sensory representations (Chadderton *et al.*, 2004). Within this model the strictly limited intensity of outgoing signalling increases the CGC layer's capacity to act as an information store (Marr, 1969; Albus, 1971). This suggests a GlyR-generated "safety catch" as the element controlling a key function of the cerebellar granule layer. In turn, the GlyRs which underwent a gain-of-function mutation, due to their higher affinity, might break the cerebellar mechanism of sensory representations' formation, storage, and translation into motor outputs.

Classical GlyR mutations which lead to hyperekplexia development are the loss-of-function mutations that reduce Cl$^-$ inhibitory current (Harvey *et al.*, 2008); it is widely accepted, that such a deficiency of inhibition provokes a massive haphazard motor activity in response to unexpected and/or uncommon sensory stimulus (Matsumoto *et al.*, 1992). On the other hand, GlyR gain-of-function mutations (with effects similar to T258F) were also shown to induce hyperekplexia (Chung *et al.*, 2010; Bode *et al.*, 2013). It seems, then, paradoxical, that mutations of opposite effect generate similar disease manifestations and full clinical syndrome. To date, the only proposed explanation is that enhanced spontaneous GlyR activity

due to gain-of-function mutation during nervous system development prevents formation of glycinergic synapses and thus induces shortage of inhibitory signaling in adult brain (Zhang *et al.*, 2016). This, however, is unlikely the case for CGCs in cerebellar vermis which are deprived of glycinergic synapses under healthy conditions. Nevertheless, it was repeatedly demonstrated that hyperekplexia is associated with functional deficits in cerebellar vermis (Leaton & Supple, 1986; Lopiano *et al.*, 1990; Goraya *et al.*, 2002). Thus one more possible explanation of cerebellar hyperekplexia mechanisms is as follows. The gain-of-function mutation, due to over-amplification of the "safety catch", disrupts the process of induction of standard activity patterns, stored in CGC layer (Chadderton *et al.*, 2004), in response to sensory inputs (as was shown in our experiment with sensory input-mimicking stimulation, Fig. 9), and thus leads to chaotic movement reactions. Alternatively, one should assume that CGCs, which are most numerous neurons in the brain and make up ~90% of neurons in cerebellum, have, nevertheless, no connection to cerebellum-associated hyperekplexia effects.

Our data demonstrate that fluctuations of GlyR-delivered tonic inhibition due to T258F mutation make a significant impact on single-receptor, single-cell and neuronal network functioning in CGC layer. The fundamental question is, however, whether modulation of GlyR inhibitory tone can lead to abnormalities at a level of a whole organism. The impact on single-cell signaling due to genetic deletion of $\alpha6$- and δ-subunits of GABA$_A$R which deprived CGCs of the major amount of tonic inhibition, was shown to be compensated by alternative signalling mechanisms (Brickley *et al.*, 2001). In line with this, genetic silencing of expression of $\alpha1$ GABA$_A$R subunit can lead to the loss of ~60% of functional GABA$_A$Rs in the brain; but, nevertheless, the connected effects on animal phenotype and behavior can be successfully compensated (Reynolds *et al.*, 2003). These observations suggest behavioral studies at animal model(s) with CGC-specific GlyR mutations as the next step in clarification of cerebellar mechanisms of hyperekplexia.

Authors contribution

C.ML. contributed to experimental work on cell cultures and edited the paper draft; J.C. performed experimental work and data analysis and produced research software; A-M.O. contributed to experimental work on cell cultures; S.S. performed experimental work, data analysis, and wrote the paper which was then critically revised by all co-authors.

Conflict of interests

Authors declare that they have no conflict of interests.

Reference list

AIBS. Allen Institute for Brain Science, Allen Brain Atlas API (2019). Available from: brain-map.org/api/index.html.

Albus JS. (1971). A theory of cerebellar function. *Mathematical Biosciences* **10,** 25-61.

Avila G, Sandoval A & Felix R. (2004). Intramembrane Charge Movement Associated with Endogenous K+ Channel Activity in HEK-293 Cells. *Cellular and Molecular Neurobiology* **24,** 317-330.

Beato M, Groot-Kormelink PJ, Colquhoun D & Sivilotti LG. (2002). Openings of the rat recombinant alpha 1 homomeric glycine receptor as a function of the number of agonist molecules bound. *The Journal of general physiology* **119,** 443-466.

Beato M, Groot-Kormelink PJ, Colquhoun D & Sivilotti LG. (2004). The activation mechanism of alpha1 homomeric glycine receptors. *The Journal of neuroscience : the official journal of the Society for Neuroscience* **24,** 895-906.

Bennett MR & Kearns JL. (2000). Statistics of transmitter release at nerve terminals. *Prog Neurobiol* **60,** 545-606.

Bi G & Poo M. (1999). Distributed synaptic modification in neural networks induced by patterned stimulation. *Nature* **401,** 792-796.

Billups D & Attwell D. (2003). Active release of glycine or D-serine saturates the glycine site of NMDA receptors at the cerebellar mossy fibre to granule cell synapse. *The European journal of neuroscience* **18,** 2975-2980.

Birnir B, Eghbali M, Cox GB & Gage PW. (2001). GABA concentration sets the conductance of delayed GABAA channels in outside-out patches from rat hippocampal neurons. *The Journal of membrane biology* **181,** 171-183.

Blednov YA, Benavidez JM, Homanics GE & Harris RA. (2012). Behavioral characterization of knockin mice with mutations M287L and Q266I in the glycine receptor alpha1 subunit. *The Journal of pharmacology and experimental therapeutics* **340,** 317-329.

Bode A, Wood SE, Mullins JG, Keramidas A, Cushion TD, Thomas RH, Pickrell WO, Drew CJ, Masri A, Jones EA, Vassallo G, Born AP, Alehan F, Aharoni S, Bannasch G, Bartsch M, Kara B, Krause A, Karam EG, Matta S, Jain V, Mandel H, Freilinger M, Graham GE, Hobson E, Chatfield S, Vincent-Delorme C, Rahme JE, Afawi Z, Berkovic SF, Howell OW, Vanbellinghen JF, Rees MI, Chung SK & Lynch JW. (2013). New hyperekplexia mutations provide insight into glycine receptor assembly, trafficking, and activation mechanisms. *The Journal of biological chemistry* **288,** 33745-33759.

Bormann J, Rundstrom N, Betz H & Langosch D. (1993). Residues within transmembrane segment M2 determine chloride conductance of glycine receptor homo- and hetero-oligomers. *The EMBO journal* **12,** 3729-3737.

Brickley SG, Revilla V, Cull-Candy SG, Wisden W & Farrant M. (2001). Adaptive regulation of neuronal excitability by a voltage-independent potassium conductance. *Nature* **409,** 88-92.

Chadderton P, Margrie TW & Häusser M. (2004). Integration of quanta in cerebellar granule cells during sensory processing. *Nature* **428,** 856.

Chen C & Okayama H. (1987). High-efficiency transformation of mammalian cells by plasmid DNA. *Molecular and cellular biology* **7,** 2745-2752.

Chung SK, Vanbellinghen JF, Mullins JG, Robinson A, Hantke J, Hammond CL, Gilbert DF, Freilinger M, Ryan M, Kruer MC, Masri A, Gurses C, Ferrie C, Harvey K, Shiang R, Christodoulou J, Andermann F, Andermann E, Thomas RH, Harvey RJ, Lynch JW & Rees MI. (2010). Pathophysiological mechanisms of dominant and recessive GLRA1 mutations in hyperekplexia. *The Journal of neuroscience : the official journal of the Society for Neuroscience* **30,** 9612-9620.

Clarkson AN, Huang BS, MacIsaac SE, Mody I & Carmichael ST. (2010). Reducing excessive GABA-mediated tonic inhibition promotes functional recovery after stroke. *Nature* **468,** 305.

Corda MG, Orlandi M, Lecca D, Carboni G, Frau V & Giorgi O. (1991). Pentylenetetrazol-induced kindling in rats: effect of GABA function inhibitors. *Pharmacology, biochemistry, and behavior* **40,** 329-333.

D'Angelo E, De Filippi G, Rossi P & Taglietti V. (1995). Synaptic excitation of individual rat cerebellar granule cells in situ: evidence for the role of NMDA receptors. *The Journal of physiology* **484 (Pt 2),** 397-413.

D'Angelo E, Rossi P, Armano S & Taglietti V. (1999). Evidence for NMDA and mGlu receptor-dependent long-term potentiation of mossy fiber-granule cell transmission in rat cerebellum. *Journal of neurophysiology* **81,** 277-287.

D'Angelo E, Rossi P, Gall D, Prestori F, Nieus T, Maffei A & Sola E. (2005). Long-term potentiation of synaptic transmission at the mossy fiber-granule cell relay of cerebellum. *Progress in brain research* **148,** 69-80.

Dzubay JA & Jahr CE. (1999). The concentration of synaptically released glutamate outside of the climbing fiber-Purkinje cell synaptic cleft. *The Journal of neuroscience : the official journal of the Society for Neuroscience* **19,** 5265-5274.

Eulenburg V & Gomeza J. (2010). Neurotransmitter transporters expressed in glial cells as regulators of synapse function. *Brain Research Reviews* **63,** 103-112.

Farrant M & Nusser Z. (2005). Variations on an inhibitory theme: phasic and tonic activation of GABA(A) receptors. *Nature reviews Neuroscience* **6,** 215-229.

Fischmeister R & Hartzell HC. (2005). Volume sensitivity of the bestrophin family of chloride channels. *The Journal of physiology* **562,** 477-491.

Flint AC, Liu X & Kriegstein AR. (1998). Nonsynaptic glycine receptor activation during early neocortical development. *Neuron* **20,** 43-53.

Flint RS, Rea MA & McBride WJ. (1981). In vitro release of endogenous amino acids from granule cell-, stellate cell-, and climbing fiber-deficient cerebella. *Journal of neurochemistry* **37,** 1425-1430.

Fujita M, Sato K, Sato M, Inoue T, Kozuka T & Tohyama M. (1991). Regional distribution of the cells expressing glycine receptor β subunit mRNA in the rat brain. *Brain Research* **560,** 23-37.

Garthwaite J & Batchelor AM. (1996). A biplanar slice preparation for studying cerebellar synaptic transmission. *Journal of neuroscience methods* **64,** 189-197.

Goraya JS, Shah D & Poddar B. (2002). Hyperekplexia in a Girl With Posterior Fossa Malformations. *Journal of Child Neurology* **17,** 147-149.

Grimwood S, Moseley AM, Carling RW, Leeson PD & Foster AC. (1992). Characterization of the binding of [3H]L-689,560, an antagonist for the glycine site on the N-methyl-D-aspartate receptor, to rat brain membranes. *Molecular pharmacology* **41,** 923-930.

Hamann M, Rossi DJ & Attwell D. (2002). Tonic and spillover inhibition of granule cells control information flow through cerebellar cortex. *Neuron* **33,** 625-633.

Hamill OP, Bormann J & Sakmann B. (1983). Activation of multiple-conductance state chloride channels in spinal neurones by glycine and GABA. *Nature* **305,** 805-808.

Harvey RJ, Topf M, Harvey K & Rees MI. (2008). The genetics of hyperekplexia: more than startle! *Trends in genetics : TIG* **24,** 439-447.

Hashimoto A, Oka T & Nishikawa T. (1995). Extracellular concentration of endogenous free D-serine in the rat brain as revealed by in vivo microdialysis. *Neuroscience* **66,** 635-643.

Hernandes MS & Troncone LRP. (2009). Glycine as a neurotransmitter in the forebrain: a short review. *Journal of Neural Transmission* **116,** 1551-1560.

Herndon RM. (1964). The fine structure of the rat cerebellum. *II The Stellate Neurons, Granule Cells, and Glia* **23,** 277-293.

Hevers W & Lüddens H. (2002). Pharmacological heterogeneity of gamma-aminobutyric acid receptors during development suggests distinct classes of rat cerebellar granule cells in situ. *Neuropharmacology* **42,** 34-47.

Huang H, Barakat L, Wang D & Bordey A. (2004). Bergmann glial GlyT1 mediates glycine uptake and release in mouse cerebellar slices. *The Journal of physiology* **560,** 721-736.

Huck S & Lux HD. (1987). Patch-clamp study of ion channels activated by GABA and glycine in cultured cerebellar neurons of the mouse. *Neuroscience letters* **79,** 103-107.

Kaneda M, Farrant M & Cull-Candy SG. (1995). Whole-cell and single-channel currents activated by GABA and glycine in granule cells of the rat cerebellum. *The Journal of physiology* **485 (Pt 2),** 419-435.

Keramidas A, Moorhouse AJ, French CR, Schofield PR & Barry PH. (2000). M2 Pore Mutations Convert the Glycine Receptor Channel from Being Anion- to Cation-Selective. *Biophysical Journal* **79,** 247-259.

Keramidas A, Moorhouse AJ, Pierce KD, Schofield PR & Barry PH. (2002). Cation-selective Mutations in the M2 Domain of the Inhibitory Glycine Receptor Channel Reveal Determinants of Ion-Charge Selectivity. *The Journal of general physiology* **119,** 393-410.

Koga T, Kozaki S & Takahashi M. (2002). Exocytotic release of alanine from cultured cerebellar neurons. *Brain Research* **952,** 282-289.

Langosch D, Thomas L & Betz H. (1988). Conserved quaternary structure of ligand-gated ion channels: the postsynaptic glycine receptor is a pentamer. *Proceedings of the National Academy of Sciences of the United States of America* **85,** 7394-7398.

Leaton R & Supple W. (1986). Cerebellar vermis: essential for long-term habituation of the acoustic startle response. *Science* **232,** 513-515.

Li P & Slaughter M. (2007). Glycine receptor subunit composition alters the action of GABA antagonists. *Visual neuroscience* **24,** 513-521.

Lopiano L, de'sperati C & Montarolo PG. (1990). Long-term habituation of the acoustic startle response: Role of the cerebellar vermis. *Neuroscience* **35,** 79-84.

Lorenzo L-E, Russier M, Barbe A, Fritschy J-M & Bras H. (2007). Differential organization of γ-aminobutyric acid type A and glycine receptors in the somatic and dendritic compartments of rat abducens motoneurons. *Journal of Comparative Neurology* **504,** 112-126.

Losi G, Prybylowski K, Fu Z, Luo JH & Vicini S. (2002). Silent synapses in developing cerebellar granule neurons. *Journal of neurophysiology* **87,** 1263-1270.

Lynch JW. (2009). Native glycine receptor subtypes and their physiological roles. *Neuropharmacology* **56,** 303-309.

Mann EO & Mody I. (2009). Control of hippocampal gamma oscillation frequency by tonic inhibition and excitation of interneurons. *Nature Neuroscience* **13,** 205.

Marr D. (1969). A theory of cerebellar cortex. *The Journal of physiology* **202,** 437-470.

Matsui T, Sekiguchi M, Hashimoto A, Tomita U, Nishikawa T & Wada K. (1995). Functional comparison of D-serine and glycine in rodents: the effect on cloned NMDA receptors and the extracellular concentration. *Journal of neurochemistry* **65,** 454-458.

Matsumoto J, Fuh P, Nigro M & Hallett M. (1992). Physiological abnormalities in hereditary hyperekplexia. *Annals of Neurology* **32,** 41-50.

Mohammadi B, Krampfl K, Cetinkaya C, Moschref H, Grosskreutz J, Dengler R & Bufler J. (2003). Kinetic analysis of recombinant mammalian alpha(1) and alpha(1)beta glycine receptor channels. *European biophysics journal : EBJ* **32,** 529-536.

Mori M, Gähwiler BH & Gerber U. (2002). β-alanine and taurine as endogenous agonists at glycine receptors in rat hippocampus in vitro. *The Journal of physiology* **539,** 191-200.

Mtchedlishvili Z & Kapur J. (2006). High-affinity, slowly desensitizing GABA$_A$ receptors mediate tonic inhibition in hippocampal dentate granule cells. *Molecular pharmacology* **69,** 564-575.

Müller T, Grosche J, Ohlemeyer C & Kettenmann H. (1993). NMDA-activated currents in Bergmann glial cells. *Neuroreport* **4,** 671-674.

Oda M, Kure S, Sugawara T, Yamaguchi S, Kojima K, Shinka T, Sato K, Narisawa A, Aoki Y, Matsubara Y, Omae T, Mizoi K & Kinouchi H. (2007). Direct correlation between ischemic injury and extracellular glycine concentration in mice with genetically altered activities of the glycine cleavage multienzyme system. *Stroke* **38,** 2157-2164.

Palay SL & Chan-Palay V. (2012). *Cerebellar cortex: cytology and organization*. Springer Science & Business Media.

Pan ZH & Slaughter MM. (1995). Comparison of the actions of glycine and related amino acids on isolated third order neurons from the tiger salamander retina. *Neuroscience* **64,** 153-164.

Pribilla I, Takagi T, Langosch D, Bormann J & Betz H. (1992). The atypical M2 segment of the beta subunit confers picrotoxinin resistance to inhibitory glycine receptor channels. *The EMBO journal* **11,** 4305-4311.

Racca C, Gardiol A & Triller A. (1998). Cell-specific dendritic localization of glycine receptor alpha subunit messenger RNAs. *Neuroscience* **84,** 997-1012.

Rajendra S, Lynch JW & Schofield PR. (1997). The glycine receptor. *Pharmacology & Therapeutics* **73,** 121-146.

Reynolds DS, O'Meara GF, Newman RJ, Bromidge FA, Atack JR, Whiting PJ, Rosahl TW & Dawson GR. (2003). GABAA α1 subunit knock-out mice do not show a hyperlocomotor response following amphetamine or cocaine treatment. *Neuropharmacology* **44,** 190-198.

Rossi DJ, Hamann M & Attwell D. (2003). Multiple modes of GABAergic inhibition of rat cerebellar granule cells. *The Journal of physiology* **548,** 97-110.

Salling MC & Harrison NL. (2014). Strychnine-sensitive glycine receptors on pyramidal neurons in layers II/III of the mouse prefrontal cortex are tonically activated. *Journal of neurophysiology* **112,** 1169-1178.

Saransaari P & Oja SS. (1993). Uptake and release of β-alanine in cerebellar granule cells in primary culture: Regulation of release by glutamatergic and gabaergic receptors. *Neuroscience* **53,** 475-481.

Sassoè-Pognetto M, Panzanelli P, Sieghart W & Fritschy JM. (2000). Colocalization of multiple GABA(A) receptor subtypes with gephyrin at postsynaptic sites. *The Journal of comparative neurology* **420,** 481-498.

Sato K, Kiyama H & Tohyama M. (1992). Regional distribution of cells expressing glycine receptor alpha 2 subunit mRNA in the rat brain. *Brain Res* **590,** 95-108.

Shan Q, Haddrill JL & Lynch JW. (2001). A single beta subunit M2 domain residue controls the picrotoxin sensitivity of alphabeta heteromeric glycine receptor chloride channels. *Journal of neurochemistry* **76,** 1109-1120.

Southam E, Morris R & Garthwaite J. (1992). Sources and targets of nitric oxide in rat cerebellum. *Neuroscience letters* **137,** 241-244.

Steinbach JH, Bracamontes J, Yu L, Zhang P & Covey DF. (2000). Subunit-specific action of an anticonvulsant thiobutyrolactone on recombinant glycine receptors involves a residue in the M2 membrane-spanning region. *Molecular pharmacology* **58,** 11-17.

Sylantyev S & Rusakov DA. (2013). Sub-millisecond ligand probing of cell receptors with multiple solution exchange. *Nature protocols* **8,** 1299-1306.

Takagi K, Ginsberg MD, Globus MY, Dietrich WD, Martinez E, Kraydieh S & Busto R. (1993). Changes in amino acid neurotransmitters and cerebral blood flow in the ischemic penumbral region following middle cerebral artery occlusion in the rat: correlation with histopathology. *Journal of cerebral blood flow and metabolism : official journal of the International Society of Cerebral Blood Flow and Metabolism* **13,** 575-585.

Takahashi T, Momiyama A, Hirai K, Hishinuma F & Akagi H. (1992). Functional correlation of fetal and adult forms of glycine receptors with developmental changes in inhibitory synaptic receptor channels. *Neuron* **9,** 1155-1161.

Takazawa T & MacDermott AB. (2010). Glycinergic and GABAergic tonic inhibition fine tune inhibitory control in regionally distinct subpopulations of dorsal horn neurons. *The Journal of physiology* **588,** 2571-2587.

Tossman U, Jonsson G & Ungerstedt U. (1986). Regional distribution and extracellular levels of amino acids in rat central nervous system. *Acta Physiologica Scandinavica* **127,** 533-545.

Traynelis SF & Jaramillo F. (1998). Getting the most out of noise in the central nervous system. *Trends in neurosciences* **21,** 137-145.

Twyman RE & Macdonald RL. (1991). Kinetic properties of the glycine receptor main- and sub-conductance states of mouse spinal cord neurones in culture. *The Journal of physiology* **435,** 303-331.

van den Pol AN & Gorcs T. (1988). Glycine and glycine receptor immunoreactivity in brain and spinal cord. *The Journal of neuroscience : the official journal of the Society for Neuroscience* **8,** 472-492.

Virginio C & Cherubini E. (1997). Glycine-activated whole cell and single channel currents in rat cerebellar granule cells in culture. *Developmental Brain Research* **98,** 30-40.

Wall MJ & Usowicz MM. (1997). Development of action potential-dependent and independent spontaneous GABAA receptor-mediated currents in granule cells of postnatal rat cerebellum. *The European journal of neuroscience* **9,** 533-548.

Wang P & Slaughter MM. (2005). Effects of GABA receptor antagonists on retinal glycine receptors and on homomeric glycine receptor alpha subunits. *Journal of neurophysiology* **93,** 3120-3126.

Wang X, Veruki ML, Bukoreshtliev NV, Hartveit E & Gerdes HH. (2010). Animal cells connected by nanotubes can be electrically coupled through interposed gap-junction channels. *Proceedings of the National Academy of Sciences of the United States of America* **107,** 17194-17199.

Watanabe E & Akagi H. (1995). Distribution patterns of mRNAs encoding glycine receptor channels in the developing rat spinal cord. *Neuroscience research* **23,** 377-382.

Westergren I, Nystrom B, Hamberger A, Nordborg C & Johansson BB. (1994). Concentrations of amino acids in extracellular fluid after opening of the blood-brain barrier by intracarotid infusion of protamine sulfate. *Journal of neurochemistry* **62,** 159-165.

Xu T-L & Gong N. (2010). Glycine and glycine receptor signaling in hippocampal neurons: Diversity, function and regulation. *Progress in Neurobiology* **91,** 349-361.

Zafra F, Gomeza J, Olivares L, Aragón C & Giménez C. (1995). Regional Distribution and Developmental Variation of the Glycine Transporters GLYT1 and GLYT2 in the Rat CNS. *European Journal of Neuroscience* **7,** 1342-1352.

Zhang LH, Gong N, Fei D, Xu L & Xu TL. (2008). Glycine uptake regulates hippocampal network activity via glycine receptor-mediated tonic inhibition. *Neuropsychopharmacology : official publication of the American College of Neuropsychopharmacology* **33,** 701-711.

Zhang Y, Bode A, Nguyen B, Keramidas A & Lynch JW. (2016). Investigating the Mechanism by Which Gain-of-function Mutations to the alpha1 Glycine Receptor Cause Hyperekplexia. *The Journal of biological chemistry* **291,** 15332-15341.

Following a BSc in genetics and cell biology and Masters in genetic engineering and novel therapeutics, Catherine gained a research position in Seth Grants' laboratory focused on genome editing with primary and differentiated cell screening to develop improved cell assay platforms.
Now based in The Roslin Institute, as part of the Gene Therapy Group, Catherines' research is concentrated on emerging genetic therapies and their optimisation for human clinical trials.

Figure 1. Affinity of GlyRs of different subunit composition to GlyR ligands. A-D: Example whole-cell responses recorded from HEK-293 cells. Dashed lines in A denote the interval where response amplitude was measured. **A:** transfection with WTα1 GlyR, effect of increasing concentrations of glycine. **B:** transfection with T258Fα1 GlyR, effect of increasing concentrations of glycine. **C:** transfection with WTα1 GlyR, effect of increasing concentrations of strychnine applied together with stable concentration of glycine. **D:** transfection with T258Fα1 GlyR, effect of increasing concentrations of strychnine applied together with stable concentration of glycine. **E-H:** Example traces recorded from nucleated patches of cultured cells. E: same as A, nucleated patch from HEK cell. F: same as B, nucleated patch from CGC. G: same as C, nucleated patch from HEK cell. H: same as D, nucleated patch from CGC. Color codes in A-H apply to sets of traces where similar solutions were used (traces to left and to right from corresponding legend). **I-L:** Example concentration-response plots for GlyR ligands with Hill's equation fitting curves; response amplitudes are normalized to maximum response. Strychnine effect was studied against EC_{50} of glycine obtained in experiments on GlyR of similar subunit composition. Refer to Tables 1 and 2 for numerical data on effects of all tested ligands at all GlyR types.
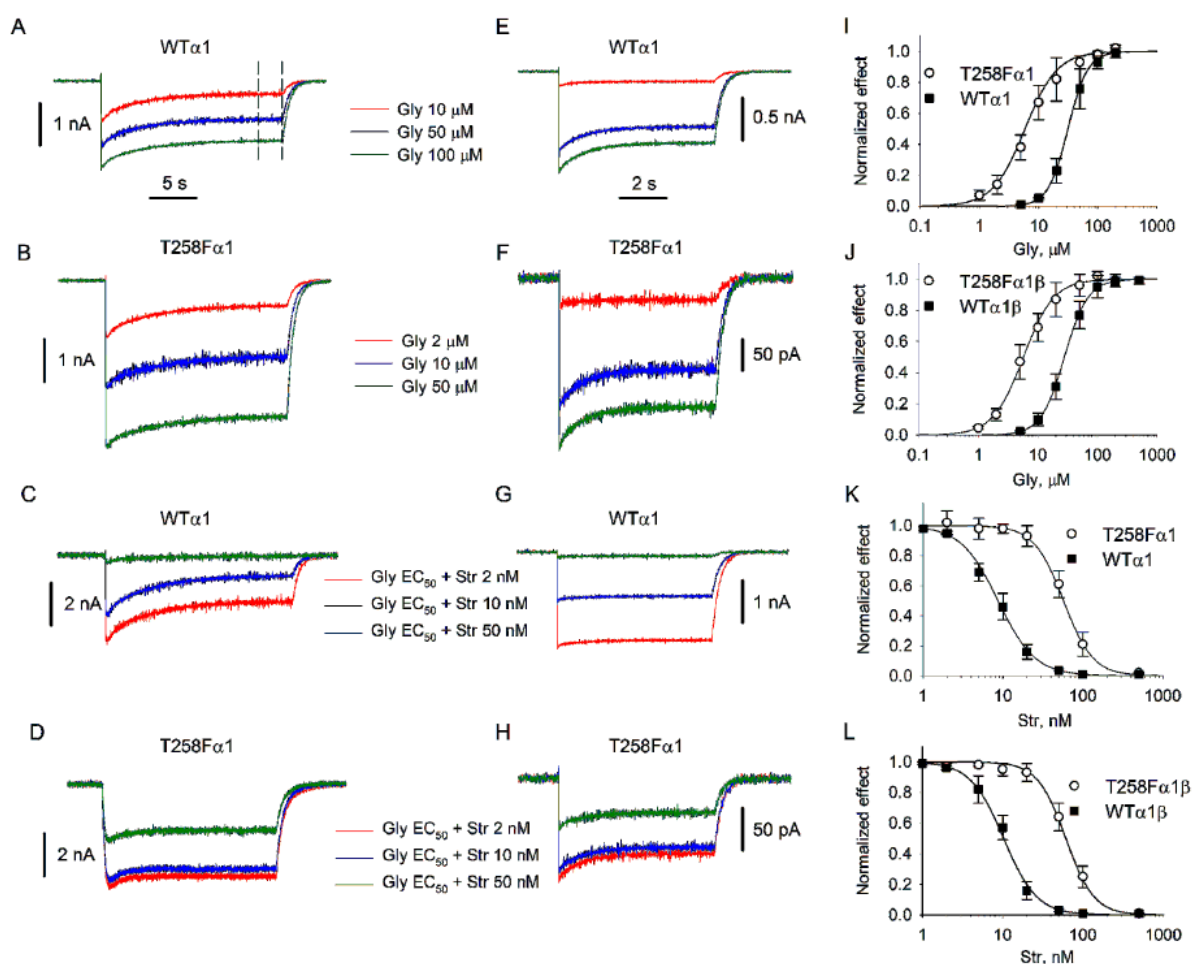

Figure 1

Figure 2. Single-channel currents generated by GlyRs of different subunit composition. A: Single-channel responses triggered by glycine application. **B:** Single-channel responses triggered by β-alanine application. From top to bottom: homomeric WTα1 GlyR, homomeric T258Fα1 GlyR, heteromeric WTα1β GlyR, heteromeric T258Fα1β GlyR. Each receptor subtype activated by EC_{50} of corresponding ligand obtained in experiment on whole cell currents. Scale bars and trace labels apply to A and B. **C:** Example all-point histograms of single-channel conductances obtained for homomeric GlyRs. Top: WTα1 GlyR. Bottom: T258Fα1 GlyR. **D:** Example all-point histograms of single-channel conductances obtained for heteromeric GlyRs. Top: WTα1β GlyR. Bottom: T258Fα1β GlyR. Refer to Table 3 for numerical data on subconductance levels revealed by Gly and Ala for different subunit compositions.
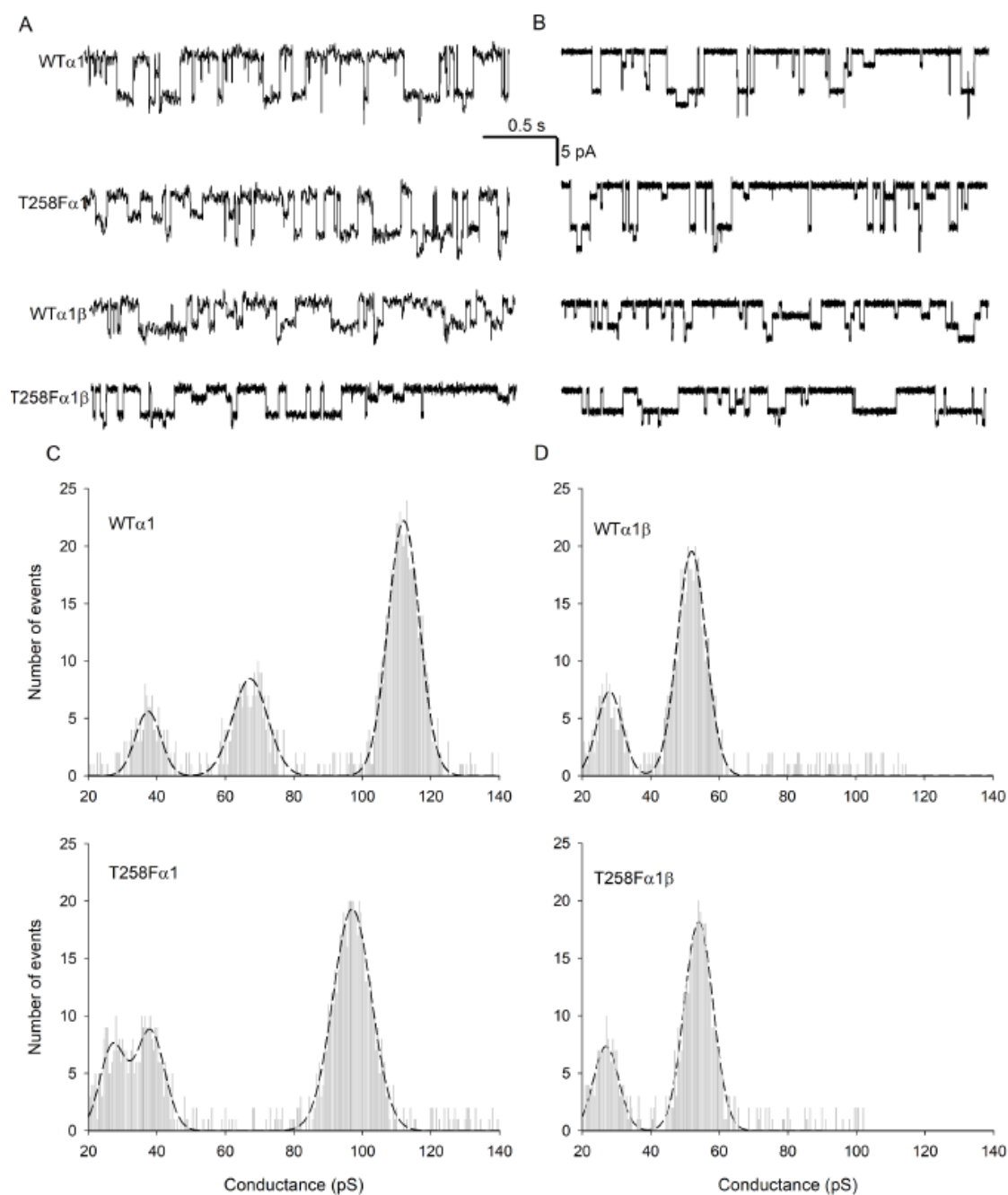

Figure 2

Figure 3 T258F mutation slowers kinetics of GlyR response triggered by brief application of agonists. A: GlyR responses evoked in HEK cell outside-out membrane patches by ~200 μs application of 1 mM glycine. Trace color codes apply to A and C. **B:** Statistical summary of A: decay time constant (τ) values of response generated by GlyRs of different subunit composition after glycine application. In B and D response amplitudes normalized to those of WTα1 receptor. **C:** GlyR responses evoked in HEK cell outside-out membrane patches by ~200 μs application of 5 mM β-alanine. **D:** Statistical summary of C: τ values of responses generated by GlyRs of different subunit composition after β-alanine application. **E:** GlyR responses evoked in CGC nucleated patches by ~200 μs application of 1 mM glycine. Response traces are normalized to peak current in non-transfected cell. **F:** Statistical summary of E: τ values of response generated by GlyRs of different subunit composition after glycine application. **G:** Images of cultured HEK cells (left) and CGCs (right). 100 μm scale bar apply to both images. * - P<0.05, n=6, Student's t-test.
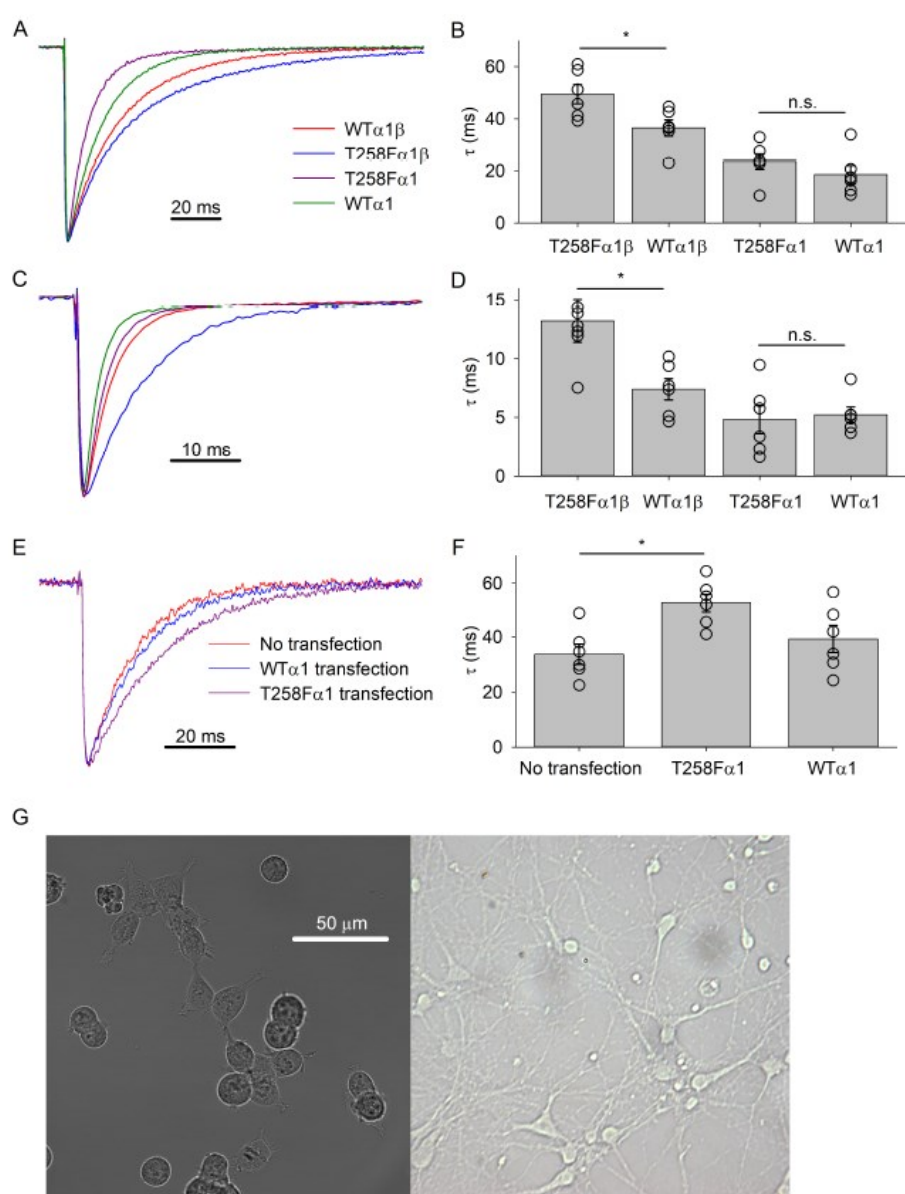

Figure 3

Figure 4. GlyR subunit composition determines response to GABA$_A$-receptor antagonists. A, B: example traces illustrating effect induced in nucleated patches by application of 10 μM glycine and glycine + GABA$_A$R antagonists. A: WTα1 subunit expressed in HEK cells. B: CGC of acute tissue. For A and B, left: effect of 10 μM picrotoxin (PTX); right: effect of 1 mM pentylenetetrazole (PTZ). Color codes apply to all example traces. **C:** Effect of 60 μM Gly + 1 mM bicuculline (BIC) on heteromeric GlyRs of various subunit composition. Left: α1β GlyRs expressed in HEK cell. Medium: α2β GlyR expressed in HEK cell. Right: nucleated patch pulled from CGC of acute cerebellar tissue. **D:** Statistical summary for A and B. Effect of Gly+PTX and Gly+PTZ on GlyR of different subunit composition expressed in HEK cells and in CGCs. Asterisk denotes significance of difference from unity. In D and E data normalized to amplitude generated by application of Gly only. E: Statistical summary of C. Asterisks denote significance of difference from both α1β and CGC columns. * - P<0.05, ** - P<0.01, n=6, Student's t-test
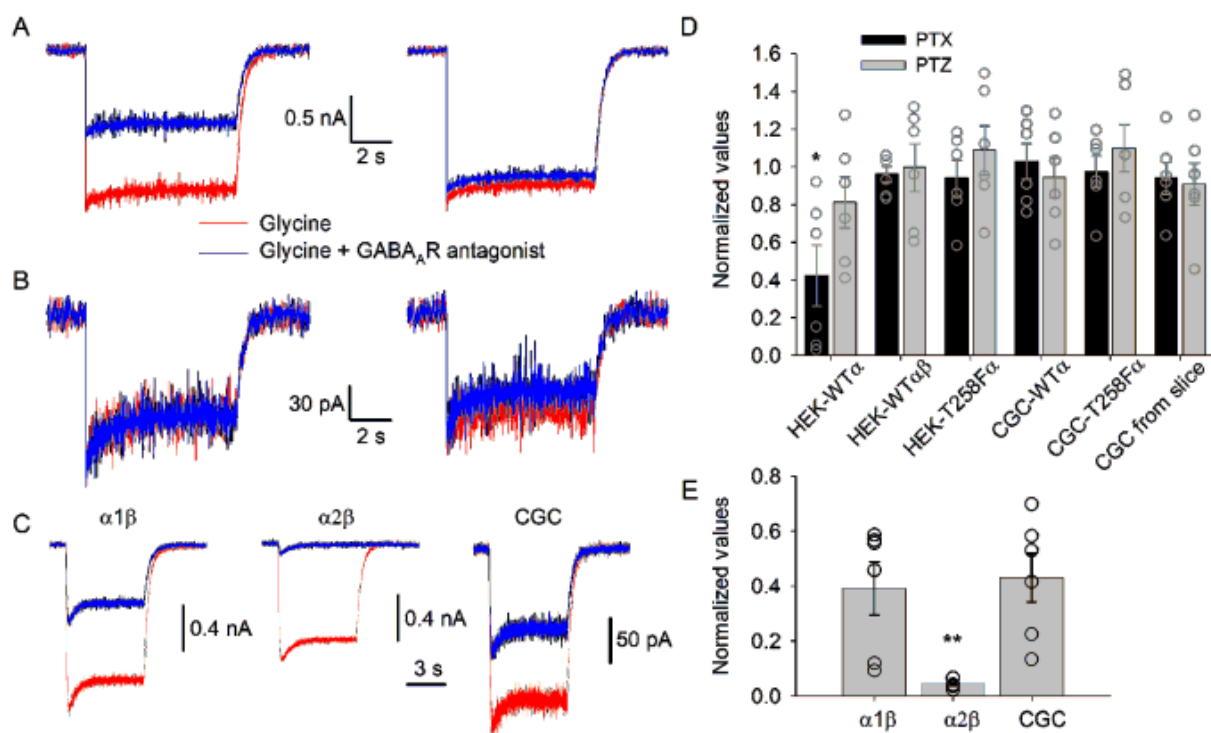

Figure 4

Figure 5. GlyRs generate significant tonic conductance in CGCs in response to enhanced release of neurotransmitters. A-C: Example traces of whole-cell recordings from CGCs in acute tissue. Dashed lines show intervals where holding current was measured, scale bars apply to all traces. **A,** from top to bottom: under control conditions, after high-frequency stimulation (HFS, 8 bursts of 10 impulses at 100 Hz) and with elevated Ca^{2+} concentration (4 mM). **B:** GlyRs of CGC remain functional with PTX, 50 µM added to perfusion solution. **C:** Strychnine does not make a significant impact on $GABA_A$Rs which are next blocked by PTX. **D:** Statistical summary of A: changes of holding current induced by 1 µM Str. **E:** Statistical summary of B: changes of holding current after HFS induced by 10 µM PTX and by 1 µM Str after PTX. **F:** Statistical summary of C: changes of holding current (with no preliminary HFS) induced by Str and by PTX after Str. Asterisks denote significance of difference from zero; *** - $P<0.001$, n=6-8, Student's paired t-test.
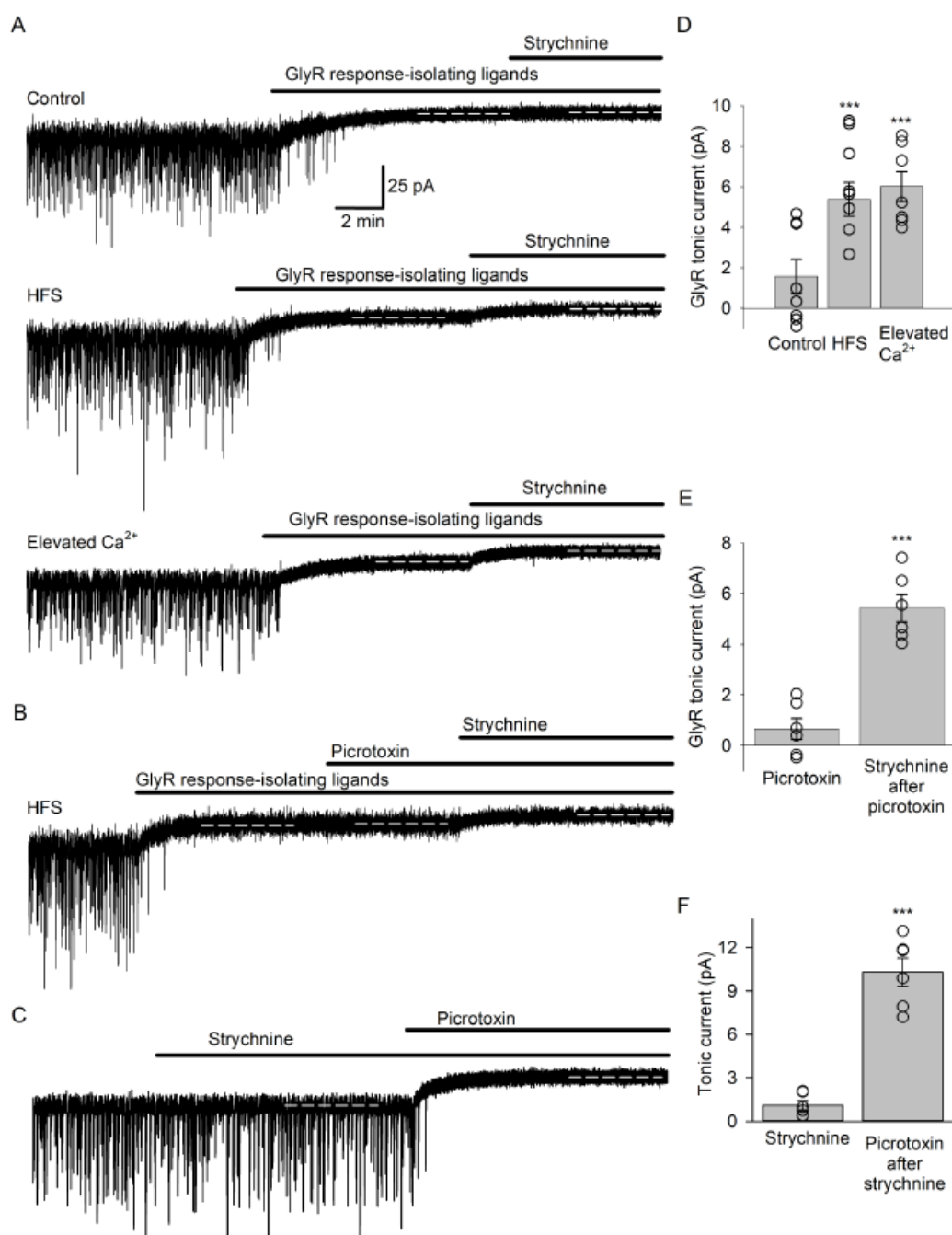

Figure 5

Figure 6 High-frequency stimulation induces release of GlyR ligands from acute tissue.
A: example traces recorded from an outside-out sniffer patch. From top to bottom: control (no stimulation), 5 μm from slice surface; control, 300 μm from slice surface; HFS, 5 μm from slice surface; HFS, 300 μm from slice surface. **B:** statistical summary. Open time fraction normalized to that obtained under control at 5 μm from slice surface. Asterisks denote significance of difference from unity, ** - P<0.01, *** - P<0.0001, n=6, paired Student's t-test.
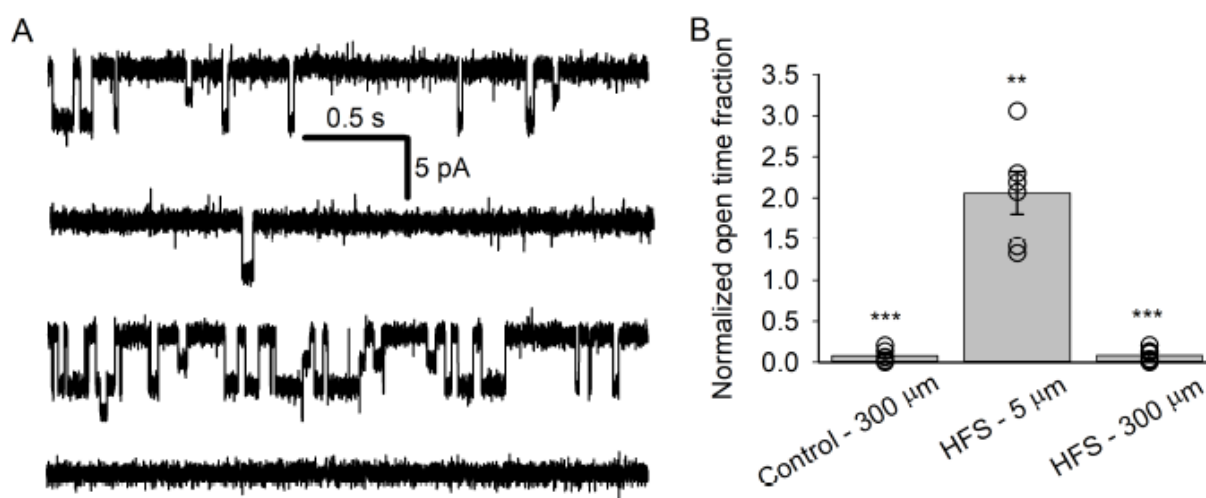

Figure 6

Figure 7. GlyRs modulate action potential generation in cultured CGCs. A-C: Example traces illustrating EPSPs evoked in CGCs by five consecutive field stimuli under control (left) and with different concentration of GlyR agonists: low (10 μM glycine or 100 μM β-alanine, medium panel) or high (50 μM glycine or 500 μM β-alanine, right panel). Stimulation artifacts are blanked; dashed lines illustrate impact of GlyR activation on EPSP amplitude; scale bars apply to all traces in A-C. **A:** No transfection. **B:** WTα1 transfection. **C:** T258Fα1 transfection. **D-E:** Statistical summary. Average number of APs generated per stimulation train under control and with different concentrations of glycine (**D**) and β-alanine (**E**). Vertical axis labels and titles on the left apply to all bar charts. Asterisks denote significance of difference from "No ligands" value. ** - P<0.01, *** - P<0.001, n=5-7, Student's t-test.
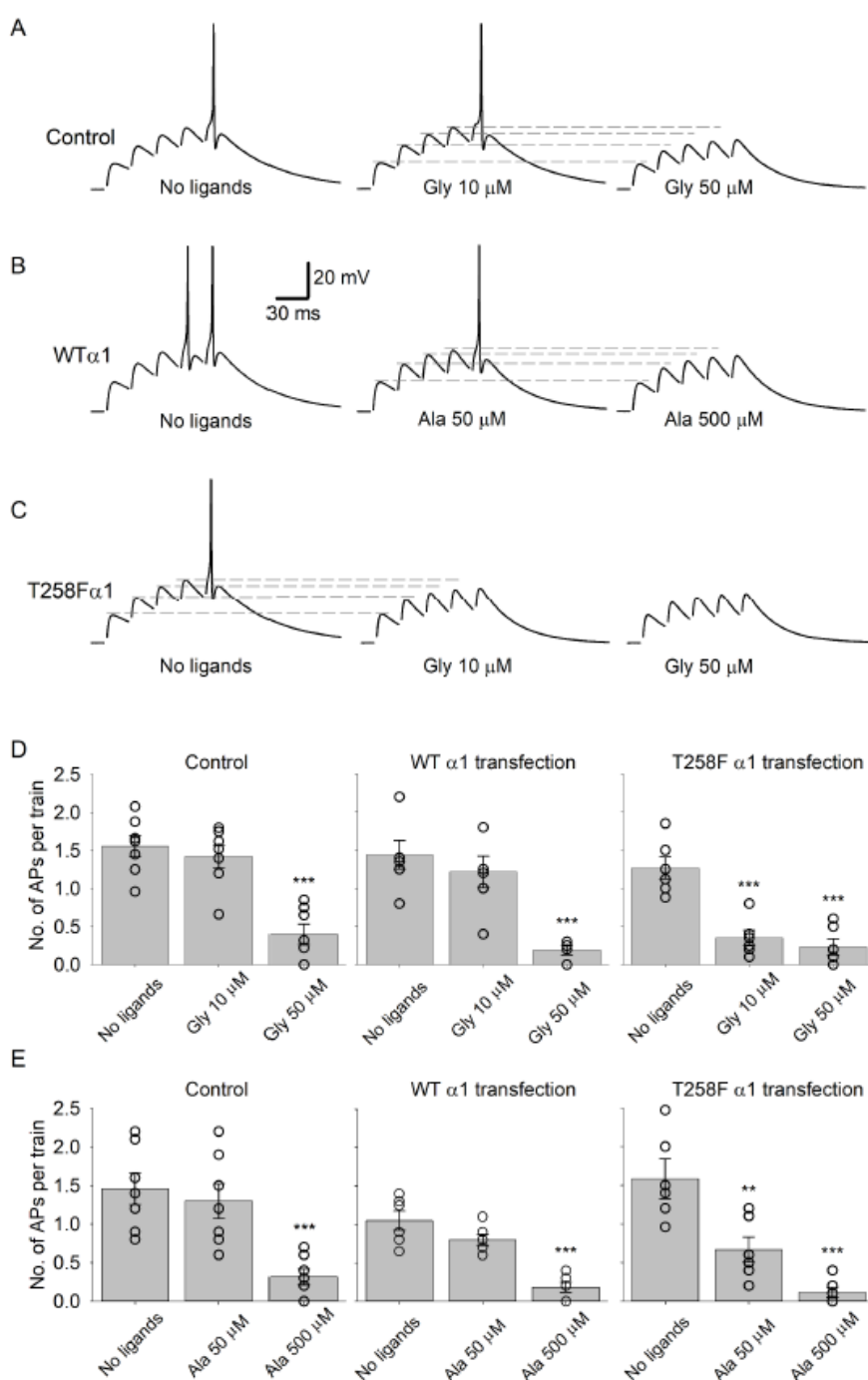

Figure 7

Figure 8. GlyRs modulate synaptic plasticity in a network of cultured CGCs. A: Sketch depicting three hypothetical polysynaptic pathways (dotted lines) leading from stimulated neuron (S) to the recorded neuron (R) with different transmission delays, corresponding to the onset latencies of the three distinct EPSC components. **B:** Traces depict 20 consecutive EPSCs (inward currents are shown upwards) recorded from a cultured neuron in response to stimulation of a nearby neuron before (left) and after repetitive paired-pulse stimulation (right). **C-F:** Statistical summary of pathway remodeling induced by paired-pulse stimulation with modulatory impact of GlyR ligands. C: Ala applied. D: Gly applied; bar color codes apply to D-F. E: Gly applied, NMDARs are blocked with 2 nM L-689,560. F: Gly applied, GlyRs are blocked with 1 µM strychnine. Asterisks denote significance of difference from "Control" value. * - P<0.05, ** - P<0.01, n=7-8, Student's t-test.
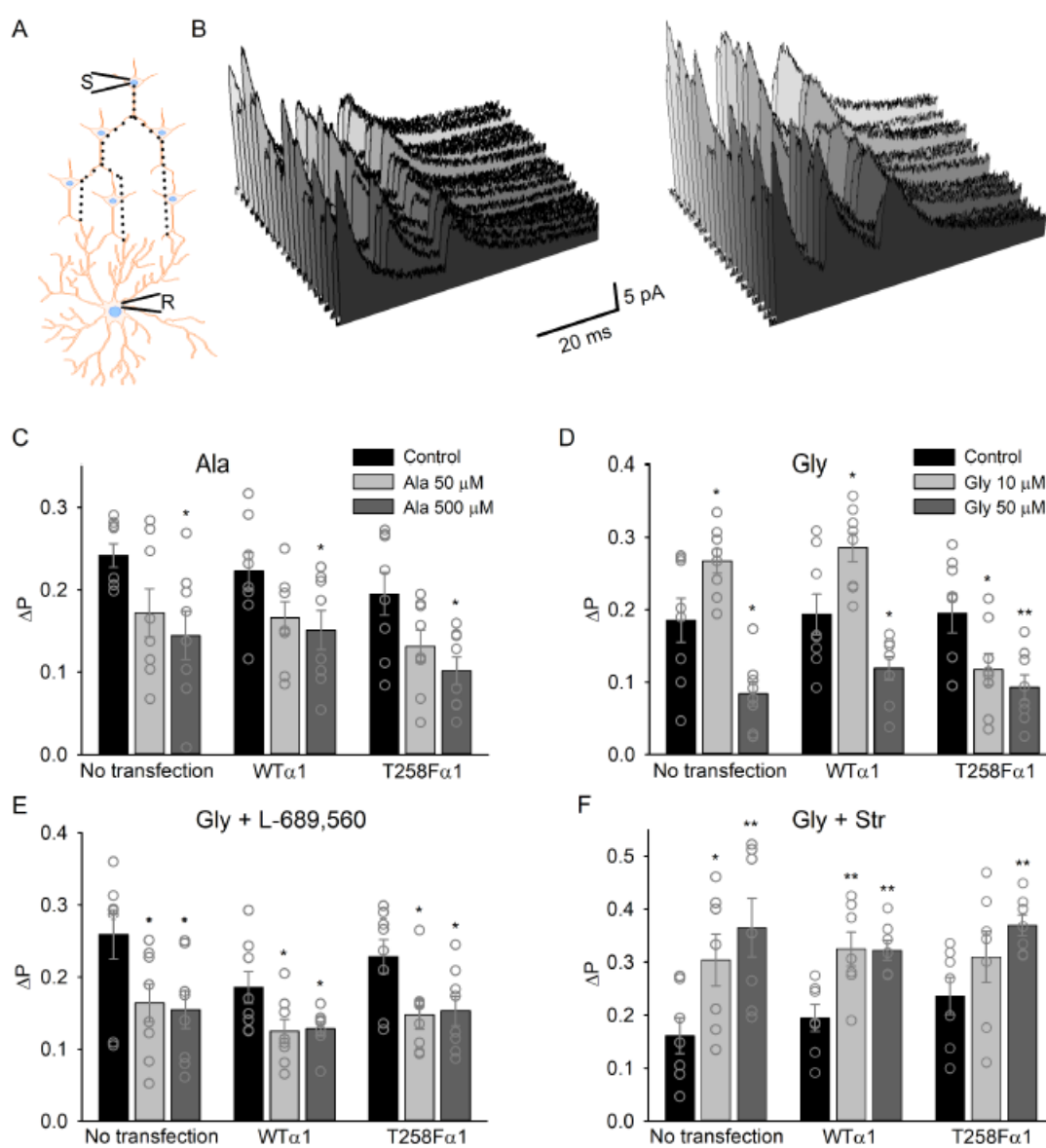

Figure 8

Figure 9. GlyRs modulate AP generation in CGCs of acute tissue. A: Examples of glutamate-evoked excitatory responses in CGC. From top to bottom: spontaneous activity; spontaneous activity and EPSC burst evoked by 5 stimuli at 25 Hz delivered through single mossy fibre; mini-EPSCs after TTX application; all activity suppressed by 50 μM NBQX application. **B:** Example action potentials evoked by 5 stimuli at 25 Hz through single mossy fibre. Top: control. Bottom: after HFS. **C:** Normalized cumulative amplitude histograms for spontaneous EPSCs, EPSCs evoked by 25 Hz stimulation, and mini-EPSCs, 1 pA bin. **D:** Statistical summary for A. Average amplitudes of spontaneous EPSCs, EPSCs evoked by 25 Hz stimulation, and mini-EPSCs, n=6 cells; 25 Hz stimulation: 10-15 episodes 30 s apart in each cell. **E-F:** Statistical summary for B. Shift in average number of APs generated by 25 Hz stimulation series: 1st stimulation set of 4 groups of 5 stimuli at 25 Hz with 30 s intervals, then 5 min interval, and 2nd stimulation set similar to the first. E: No HFS. Left: control. Right: Gly 50 μM added after 1st stimulation set. F: HFS after the 1st stimulation set. Left: control. Right: strychnine 1 μM added after the 1st stimulation set. Bar titles and vertical axes titles apply to all bar charts in E-F. Asterisks denote significance of difference between average number of APs in 1st and 2nd stimulation set; ** - P<0.01, *** - P<0.001, n=9-11, Student's paired t-test.
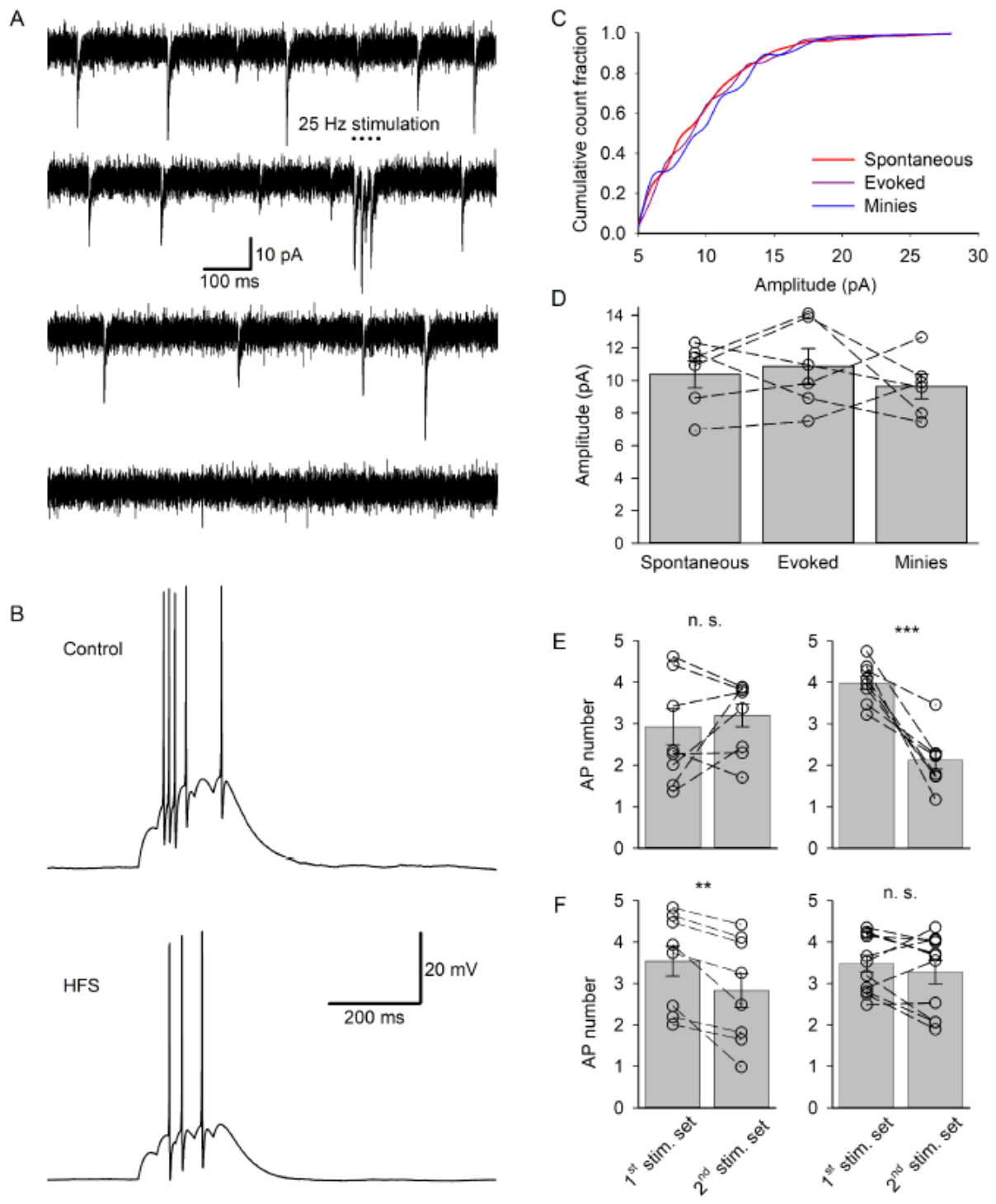
Figure 9

Table 1. Pharmacology of GlyRs of different subunit composition expressed in HEK-293 cells, mean±SE, whole-cell recordings. Values calculated for equilibrated current; EC_{50} and IC_{50} values obtained for peak current are given in brackets.

GlyR subunit composition	Glycine			β-Alanine			Strychnine vs. Glycine[a]			Strychnine vs. β-Alanine[a]		
	EC_{50}, μM	n_h	n	EC_{50}, μM	n_h	n	IC_{50}, nM	n_h	n	IC_{50}, nM	n_h	n
WTα1	32.3±2.1 (26.1±17.3)	2.6±0.3	6	267±43.8 (318±141)	2.3±0.2	6	8.7±1.8 (13.2±6.4)	1.9±0.6	6	7.6±1.3 (9.6±1.8)	2.2±0.2	5
T258Fα1	6.8±1.1 (11.3±6.2)	1.7±0.2	6	70±13.2 (92.3±48.6)	1.8±0.3	6	52.6±8.7 (39.5±19.8)	2.3±0.5	6	34.1±7.4 (22.5±11.7)	2.4±0.5	6
WTα1β	18.8±2.9 (13.8±8.7)	2.2±0.2	7	142±14.1 (206±117)	2.2±0.4	5	10.3±2.1 (24.1±16.7)	2.1±0.7	6	7.4±1.6 (8.3±4.3)	2.0±0.4	6
T258Fα1β	8.1±0.9 (14.1±7.6)	1.5±0.1	6	77±12.8 (104±56.4)	1.9±0.3	7	59.8±8.6 (88.3±36.2)	2.6±0.7	5	42.6±8.9 (31.4±11.9)	2.1±0.3	5

[a]-Agonist concentration equals EC_{50} obtained when pure agonist (glycine or β-alanine) was tested at GlyRs of correspondent subunit composition.

Table 2. Pharmacology of GlyRs of different subunit composition expressed in HEK-293 cells and in CGCs, mean±SE, recordings from nucleated patches. Values calculated for peak current.

GlyR subunit composition, cell type	Glycine			Strychnine vs. Glycine[b]		
	EC_{50}, μM	n_h	n	IC_{50}, nM	n_h	n
WTα1β, HEK	20.3±1.8	1.9±0.1	5	8.4±1.8	2.0±0.4	5
T258Fα1β, HEK	7.9±1.2	1.4±0.2	5	49.6±7.6	2.8±0.5	5
WTα1, CGC	21.2±1.9	2.1±0.2	5	7.8±2.2	1.9±0.3	5
T258Fα1, CGC	8.5±0.6	1.7±0.3	6	52.6±4.3	2.2±0.2	5
Living tissue, CGC	24.5±3.2	2.3±0.4	5	9.3±2.9	2.2±0.4	5

[b]-Glycine concentration equals EC_{50} obtained when pure glycine was tested at GlyRs of correspondent subunit composition.

Table 3. Conductance states and their input into overall charge transfer for GlyRs expressed in HEK-293 cells and recorded from outside-out patches, mean±SE. Agonists concentration equals EC_{50} obtained in whole cell for correspondent subunit composition; n=6 for glycine, n=7 for β-alanine.

GlyR subunit composition	Agonist			
	Glycine		β-Alanine	
GlyR subunit composition	**Conductance states (pS)**	**Charge transfer (%)[c]**	**Conductance states (pS)**	**Charge transfer (%)[c]**
WTα1	112±3.6, 67±1.8, 37±2.4	86.2, 9.7, 3.3	108±2.2, 71±2.3, 32±2.7	87.3, 8.4, 2.2
T258Fα1	97±2.9, 38±4.1, 27±3.3	92.1, 2.8, 4.8	95±1.4, 46±2.8, 19±2.7	91.3, 2.5, 5.1
WTα1β	52±1.9, 28±2.6	88.6, 8.8	56±2.8, 25±2.7	92.7, 5.4
T258Fα1β	54±2.5, 27±1.7	90.3, 7.9	51±3.1, 29±2.3	89.6, 8.2

[c]-Sum of values may be <100% due to high-amplitude noise events.

Table 4. Conductance states and their input into overall charge transfer for GlyRs expressed in CGCs and activated by glycine in outside-out patches, mean±SE. For WTα1 and T258Fα1 overexpressed in cultured CGCs glycine concentration equals EC$_{50}$ obtained in HEK-293 cells for correspondent subunit composition. Data for living tissue were obtained in a sniffer patch experiment, n=6 for all experiments.

GlyR subunit composition	Conductance states (pS)	Charge transfer (%)[d]
Transfected with WTα1	56±2.6, 30±2.2	94.8, 4.6
Transfected with T258Fα1	51±3.1, 28±2.3	87.2, 9.1
Living tissue	57±1.8, 29±3.1	90.1, 8.8

[d]-Sum of values may be <100% due to high-amplitude noise events.